National Défense
Defence nationale

UNCLASSIFIED
UNLIMITED DISTRIBUTION

DREV REPORT 4351/85
FILE: 3633B-007
MARCH 1985

CRDV RAPPORT 4351/85
DOSSIER: 3633B-007
MARS 1985

LASER FORWARD- AND BACKSCATTERING IN PARTICULATE MEDIA

L.R. Bissonnette

BUREAU - RECHERCHE ET DÉVELOPPEMENT
MINISTÈRE DE LA DÉFENSE NATIONALE
CANADA

RESEARCH AND DEVELOPMENT BRANCH
DEPARTMENT OF NATIONAL DEFENCE
CANADA

NON CLASSIFIÉ
DIFFUSION ILLIMITÉE

Canada

85-3677/

DREV R-4351/85
FILE: 3633B-007

UNCLASSIFIED

CRDV R-4351/85
DOSSIER: 3633B-007

LASER FORWARD- AND BACKSCATTERING IN PARTICULATE MEDIA

by

L.R. Bissonnette

CENTRE DE RECHERCHES POUR LA DEFENSE

DEFENCE RESEARCH ESTABLISHMENT

VALCARTIER

Tel: (418) 844-4271

Québec, Canada

March/mars 1985

NON CLASSIFIE

ABSTRACT

A model of optical and infrared wave propagation in scattering media is derived from Maxwell's equations. It allows for the calculation of the irradiance profiles of the forward- and the backward-propagating beams which result from the interaction of a coherent beam with a scattering medium. The method accounts for all orders of scattering and is applicable to inhomogeneous media. The range of validity is limited by the condition that the fractional volume occupied by the particles to the $\frac{1}{3}$th power must be much smaller than unity.

RÉSUMÉ

On a mis au point, à partir des équations de Maxwell, un modèle de propagation des ondes optiques et infrarouges dans un milieu diffusant. Ce modèle permet de calculer les profils de l'intensité lumineuse des faisceaux se propageant vers l'avant et vers l'arrière et qui résultent de l'interaction d'un faisceau coherent avec les particules. La méthode tient compte de tous les ordres de diffusion et peut s'appliquer aux milieux inhomogènes. Le domaine de validité est limité par la condition suivante: la fraction du volume occupé par les particules à la puissance $\frac{1}{3}$ doit être beaucoup plus petite que l'unité.

TABLE OF CONTENTS

ABSTRACT/RÉSUMÉ 1

LIST OF SYMBOLS v

1.0 INTRODUCTION 1

2.0 THEORETICAL BACKGROUND 2

3.0 STOCHASTIC APPROACH 5

4.0 MODEL 11

4.1 Source-Sink Terms 11
4.2 Hypotheses 12
4.3 Constitutive Relations 14
4.4 Propagation Coefficients 19

5.0 PROPAGATION EQUATIONS 29

6.0 BEAM WAVES 30

7.0 PLANE WAVES 39

8.0 CONCLUSION 46

9.0 REFERENCES 48

FIGURES 1 to 7

LIST OF SYMBOLS

Notation	Description	Defining Equation
A	Complex wave amplitude	4
A_b	Complex wave amplitude of backward-propagating wave	8
A_c	Coherent part of complex wave amplitude	14
A_f	Complex wave amplitude of forward-propagating wave	7
A_r	Average reduced amplitude	94
D_{4b}	Diffusion tensor of backward-propagating scattered irradiance	69
D_b	Diffusion coefficient of backward-propagating scattered irradiance	93
D_{4f}	Diffusion tensor of forward-propagating scattered irradiance	68
D_f	Diffusion coefficient of forward-propagating scattered irradiance	93
E	Wave electric field	1
$\hat{E}$	Temporal Fourier transform of wave electric field	
F	Focal distance of unperturbed beam	36
G_b	Covariance function of backscattered wave amplitude	70
G_f	Covariance function of forward-scattered wave amplitude	71
H	Covariance function of the exponential of the phase difference between the backscattered waves from the forward- and the backward-propagating waves	72
I^+	Forward-propagating scattered irradiance	95
I^-	Backward-propagating scattered irradiance	96
L	Longitudinal correlation scale of the forward phase front angle fluctuations	75
L^-	Longitudinal correlation scale of the backward phase front angle fluctuations	78

L_H	Longitudinal correlation scale of the covariance function H	88
M,N	Dummy functions	91
O^+, O^-	Integral operators	54, 55
P_b, P_f	Phase structure functions of backscattered waves from the backward-propagating and forward-propagating waves	86
S	Source-sink term arising from interaction of the forward- and the backward-propagating waves through the particles	1
$\tilde{S}$	Temporal Fourier component of S	
$\tilde{S}_b$	Temporal Fourier component of source-sink term in equation for backward-propagating wave amplitude	7, 29
$\tilde{S}_f$	Temporal Fourier component of source-sink term in equation for forward-propagating wave amplitude	8, 30
U,W	Functions of the random index of refraction	9, 10
$\underset{\sim}{V}_b$	Geometric phase front angle of backward-propagating wave	5
$\underset{\sim}{V}_f$	Geometric phase front angle of forward-propagating wave	6
Z	Physical thickness of scattering cloud	
a	Random part of A	14
a_b	Random part of A_b	
a_f	Random part of A_f	
<b>	Average particle size	
c	Speed of light in free space	
g_b, g_f	Substituting functions	38, 39
h	Dummy function	54, 55
i	$= \sqrt{-1}$	
k	Optical wave number	4
ℓ	Transverse correlation scale of the forward phase front angle fluctuations	76
$\bar{\ell}$	Transverse correlation scale of the backscattered phase front angle fluctuations	77

ℓ_H	Transverse correlation scale of the covariance function H	87
n	Random field of the complex refractive index of the particulate medium	3
n_r, n_i	Real and imaginary parts of n	
n_{ro}, n_{io}	Real and imaginary parts of reference refractive index	
n_p	Real part of the complex refractive index of a particle	
r	Transverse coordinate	
t	Time	
u,w	Random part of U and W	11, 12
$\underset{\sim}{V}_b, \underset{\sim}{V}_f$	Random part of $\underset{\sim}{V}_b$ and $\underset{\sim}{V}_f$	13
z	Longitudinal coordinate	
A_b, A_f	Particle absorption functions	56, 57
Λ	Similarity parameter	107
Π	Ratio of backscattering to total scattering coefficients	125
Ω	Single-scattering albedo of the particulate medium	124
α	Similarity parameter	108
β	Similarity parameter	109
γ	Exit angle of primary refracted ray from a homogeneous spherical particle, relative to direction of incidence	81, Fig.1
$\underset{\sim}{\delta}$	Two-dimensional unit dyad	
δ	Function of Π and Ω	128
ε	Function of Π and Ω	129
ε'	Relative dielectric constant	
ζ	Optical thickness of cloud	117
η	Optical depth	100
θ	Incidence angle of ray impinging on a spherical particle	Fig. 1

κ_b, κ_f	Similarity parameters	111, 112
λ	Radiation wavelength	
μ'	Relative magnetic permeability	
ν	Particle number density	
π	= 3.14159.....	
ρ	Normalized transverse coordinate	101
σ_a	Main contribution to particle absorption coefficient	97
σ_{ab}	Second-order contribution to particle absorption coefficient for backward-propagating average amplitude	59
σ_{af}	Second-order contribution to particle absorption coefficient for forward-propagating average amplitude	58
σ_{abs}	Second-order contribution to particle absorption coefficient for backward-propagating average scattered irradiance	61
σ_{afs}	Second-order contribution to particle absorption coefficient for forward-propagating average scattered irradiance	60
σ_{cb}	Forward-scattering coefficient of backward-propagating average amplitude	63
σ_{cf}	Forward-scattering coefficient of forward-propagating average amplitude	62
$\bar{\sigma}_{cb}$	Backscattering coefficient of backward-propagating average amplitude	65
$\bar{\sigma}_{cf}$	Backscattering coefficient of forward-propagating average amplitude	64
$\bar{\sigma}_{sb}$	Backscattering coefficient of backward-propagating average scattered irradiance	67
$\bar{\sigma}_{sf}$	Backscattering coefficient of forward-propagating average scattered irradiance	66

σ_t	Total single scattering coefficient	102
τ	Similarity parameter	110
ϕ	Angle of primary reflected ray relative to direction of incidence	79, Fig. 1
χ	Similarity parameter	106
ψ	Exit angle of primary internally reflected ray from a homogeneous spherical particle, relative to direction of incidence	80
ω	Optical frequency of radiation	
∂	Partial derivative	
$\underset{\sim}{\nabla}$	Three-dimensional gradient operator	
$\underset{\sim}{\nabla}_\perp$	Gradient operator in transverse plane	
$\underset{\sim}{\nabla}_\rho$	Gradient operator in nondimensional transverse coordinates	
$< >$	Ensemble average	

1.0 INTRODUCTION

A characteristic feature of modern warfare is the widespread use of electro-optical systems designed to enhance the effectiveness of various weapons. However, poor weather conditions and/or artificial obscurants can severely degrade their performance. Hence, a requirement exists for understanding and predicting the propagation of electromagnetic waves under adverse conditions created mostly by the presence of suspended natural or man-made aerosols.

Propagation in thin or tenuous clouds is well understood and documented (Refs. 1 and 2). It is governed by simple and exact single-scattering equations which explain numerous atmospheric phenomena. However, for military applications, there are many instances of low visibility conditions where the single scattering hypothesis fails. In such dense clouds, the optical rays undergo many scattering events before escaping the medium, reaching a target, or being detected. These multiple scatterings have nonnegligible and often dominant effects on the propagated wave. Analytic methods (e.g. Refs. 3-5), transport methods (e.g. Refs. 6-15), and Monte Carlo simulations (e.g. Refs. 16-17) have all been used to study this problem. The mathematics are complex and no general solution has been obtained yet. The numerical analysis based on the Monte Carlo method is time-consuming and provides empirical relations only. Fortunately, there are special and practical cases where simplifications are possible, which result in useful approximate theories. The most accurate of these approaches was developed at Defence Research Establishment Valcartier (DREV) (Refs. 11-15). It consists of the exact series solution of the small-angle approximation to the radiative transfer equation. The model is very convenient for numerical computations and gives valuable insight into the relative effects of the various scattering orders. However, it is restricted to homogeneous media and it does not appear readily applicable to the important inverse problem of interpreting lidar measurements for the determination of the optical properties of the medium.

A model based on a different theoretical approach is developed here. It stems from the Maxwell's equations of electromagnetic wave propagation and not from the radiative transfer equation. The method predicts the irradiance profiles of the forward- and backscattered beams including the lidar configuration. All orders of scattering are accounted for but they are not individually identified. The theoretical basis is outlined in Chapter 2.0. Chapter 3.0 describes the stochastic approach. The original features of the model are introduced and discussed in Chapter 4.0, and Chapter 5.0 gives the resulting propagation equations. Sample solutions for beam waves and plane waves are derived and analysed in Chapters 6.0 and 7.0 respectively.

This work was performed at DREV between January and December 1983 under PCN 33B07, Atmospheric Propagation of Laser Beams.

2.0 THEORETICAL BACKGROUND

The object of this work is to describe the propagation of the forward- and backward-going electromagnetic waves in a particulate medium. We restrict the analysis to situations where polarization effects are negligible. Under this approximation, the wave electric field E can be considered scalar and, from Maxwell's equations, it satisfies the equation

$$\nabla^2 E - \frac{\partial^2}{\partial t^2}\left[\frac{(\mu'\varepsilon')}{c^2} E\right] = S, \qquad [1]$$

where ∇^2 is the three-dimensional Laplacian operator, t is the time, μ' is the relative magnetic permeability, ε' is the relative dielectric constant of the medium, and c is the speed of light in free space. The right-hand-side function S is the source-sink term arising from the interaction of the forward- and backward-propagating waves through the particles in the medium. S is related to the current and charge densities induced on or within the particles. However, it will not be

formulated in this exact fashion here; it will be modeled as described later in Section 4.1.

We consider only one temporal Fourier component of the electric field. If ω denotes the angular frequency of the wave, the temporal Fourier transform of eq. 1 yields

$$\nabla^2 \tilde{E} - \frac{(\mu'\varepsilon')\omega^2}{c^2} \tilde{E} = \tilde{S}, \qquad [2]$$

where the tilde ($\sim$) denotes a Fourier transform. Equation 2 was simplified through the approximation $\omega >> (\mu'\varepsilon')^{-1} \frac{\partial(\mu'\varepsilon')}{\partial t}$ which is well justified for optical and infrared waves. The product $(\mu'\varepsilon')$ is the square of the complex refractive index n and it is written

$$\mu'\varepsilon' = n^2. \qquad [3]$$

We seek a solution of the form

$$\tilde{E} = A \exp\left[ik(\hat{z}z + \phi)\right], \qquad [4]$$

where z is the coordinate along the main direction of propagation, $i = \sqrt{-1}$, $k^2 = \omega^2(n_{ro}^2 - n_{io}^2)/c^2$ is the wave number, n_{ro} and n_{io} are respectively the real and imaginary parts of the reference refractive index, and A and ϕ are functions to be specified below. On substituting eq. 4 for $\tilde{E}$ in eq. 2, we obtain after separation

$$\frac{\partial \underset{\sim}{V}_f}{\partial z} + \underset{\sim}{V}_f \cdot \underset{\sim}{\nabla}\, \underset{\sim}{V}_f = \underset{\sim}{\nabla}\, U, \qquad [5]$$

$$-\frac{\partial \underset{\sim}{V}_b}{\partial z} + \underset{\sim}{V}_b \cdot \underset{\sim}{\nabla}\, \underset{\sim}{V}_b = \underset{\sim}{\nabla}\, U, \qquad [6]$$

$$\frac{\partial A_f}{\partial z} + \underset{\sim}{V}_f \cdot \underset{\sim}{\nabla} A_f + \frac{1}{2} A_f \underset{\sim}{\nabla} \cdot \underset{\sim}{V}_f + kW A_f - \frac{i}{2k} \nabla^2 A_f = \tilde{S}_f e^{-ik(z+\phi_f)}, \quad [7]$$

$$-\frac{\partial A_b}{\partial z} + \underset{\sim}{V}_b \cdot \underset{\sim}{\nabla} A_b + \frac{1}{2} A_b \underset{\sim}{\nabla} \cdot \underset{\sim}{V}_b + kWA_b - \frac{i}{2k} \nabla^2 A_b = \tilde{S}_b e^{-ik(z+\phi_b)}, \quad [8]$$

where the subscripts f and b refer to the forward and the backward wave respectively, and where $\underset{\sim}{V}_f \equiv \underset{\sim}{\nabla}\phi_f$ and $\underset{\sim}{V}_b \equiv \underset{\sim}{\nabla}\phi_b$. The functions U and W are defined as follows:

$$U = \frac{n_r^2 - n_i^2 - n_{ro}^2 + n_{io}^2}{n_{ro}^2 - n_{io}^2}, \quad [9]$$

$$W = \frac{n_r n_i}{n_{ro}^2 - n_{io}^2}, \quad [10]$$

where n_r and n_i are the real and imaginary parts of the instantaneous and local complex refractive index of the particulate medium.

Two types of separation were performed in obtaining eqs. 5-8; first, the separation into the forward and the backward waves which has its basis in the + and - signs in eq. 4, and second, the separation into an equation for the phase front angle $\underset{\sim}{V}$ and the amplitude A. The latter separation is different from the more common practice of factoring out the real and imaginary parts in eq. 2. The basis is to uncouple the equation of $\underset{\sim}{V}$ (or ϕ) from that of the complex amplitude A.

Equations 5 and 6 are the eikonal equations, or the geometric optics equations, of the forward and backward waves. The surfaces $(z+\phi)$ = constants are the geometric phase fronts and the vector $(\underset{\sim}{V} + \underset{\sim}{k})$ gives the direction of the optical rays, where $\underset{\sim}{k}$ is the unit vector along the z-axis. Hence, from eqs. 4, 7 and 8, it follows that A is

the complex amplitude defined on the geometric phase front. This complex amplitude embodies the phase perturbations induced by diffraction.

3.0 STOCHASTIC APPROACH

For the present analysis, we model the particulate medium as a space-time random function of the complex index of refraction n. This function can be specified from the given properties of the medium, i.e. the number density of the particles, their shape, their size distribution, the distributed complex refractive index within the particles, and the complex refractive index of the surrounding medium. Hence, the quantities $\underset{\sim}{V}$ and A are random functions and the governing eqs. 5-8 are stochastic equations.

There is no known general method of solving for the random functions $\underset{\sim}{V}$ and A. In any case, this would yield much more information than is required in practice. The quantities of interest are the averages and one possible approach consists in using the stochastic eqs. 5-8 to derive deterministic equations for these averages or statistical moments. In the present application, we are interested in the moments $\langle A \rangle$ and $\langle AA^* \rangle$ which are respectively the average field amplitude and the average irradiance.

The method of derivation is as follows. First, the functions U and W representing the medium properties are written as sums of an average and a random part, i.e.

$$U = \langle U \rangle + u \; ; \; \langle u \rangle = 0, \qquad [11]$$

$$W = \langle W \rangle + w \; ; \; \langle w \rangle = 0, \qquad [12]$$

where the pointed brackets denote ensemble averaging. The same decomposition is performed for the dependent wave front function

$$\underset{\sim}{V} = \langle \underset{\sim}{V} \rangle + \underset{\sim}{v} \; ; \; \langle \underset{\sim}{v} \rangle = 0. \qquad [13]$$

The field amplitude A is separated in a slightly different way into a coherent (subscript c) and an incoherent (lower case letter) contribution

$$A = A_c + a \; ; \; \langle a \rangle = 0. \qquad [14]$$

The component a is random and represents the scattered amplitude. The component A_c is not fully deterministic. There are randomly distributed holes in the profile of A_c left by the presence of the scatterers.

If we substitute eqs. 12-14 for W, $\underset{\sim}{V}$ and A_f in eq. 7 and drop the subscript f for brevity, we obtain

$$\frac{\partial A_c}{\partial z} + \frac{\partial a}{\partial z} + \langle \underset{\sim}{V} \rangle \cdot \underset{\sim}{\nabla} A_c + \langle \underset{\sim}{V} \rangle \cdot \underset{\sim}{\nabla} a + \underset{\sim}{v} \cdot \underset{\sim}{\nabla} A_c + \underset{\sim}{v} \cdot \underset{\sim}{\nabla} a$$

$$+ \frac{1}{2} A_c \, \underset{\sim}{\nabla} \cdot \langle \underset{\sim}{V} \rangle + \frac{1}{2} a \, \underset{\sim}{\nabla} \cdot \langle \underset{\sim}{V} \rangle + \frac{1}{2} A_c \, \underset{\sim}{\nabla} \cdot \underset{\sim}{v} + \frac{1}{2} a \, \underset{\sim}{\nabla} \cdot \underset{\sim}{v}$$

$$+ k \langle W \rangle A_c + k \langle W \rangle a + k w A_c + k w a$$

$$- \frac{i}{2k} \nabla^2 A_c - \frac{i}{2k} \nabla^2 a = \tilde{S} \, e^{-ik(z+\phi)}. \qquad [15]$$

The terms of the form $\underset{\sim}{V} \cdot \underset{\sim}{\nabla} A$ are transport terms. They account for the propagation of the amplitude A along the rays of direction $(\underset{\sim}{k}+\underset{\sim}{V})$. The terms $\frac{1}{2} A \, \underset{\sim}{\nabla} \cdot \underset{\sim}{V}$ represent the compressibility of the amplitude. A increases if the rays converge and decreases if they diverge. According to this general interpretation, we can set in eq. 15

$$\underset{\sim}{v} \cdot \nabla A_c = 0, \qquad [16]$$

which states that the coherent amplitude is not propagated by the incoherent or scattered rays. Physically, this is explained by the fact that $A_c = 0$ immediately past the particles so that it cannot be transported by the scattered rays that originate from the particles. On the other hand, the term $\frac{1}{2} A_c \underset{\sim}{\nabla} \cdot \underset{\sim}{v}$ is not zero instantaneously since it models the action of the scattering rays on the nonzero coherent amplitude that impinges on the particles. The term $\frac{1}{2} A_c \underset{\sim}{\nabla} \cdot \underset{\sim}{v}$ is responsible for the depletion of the coherent amplitude, i.e. its transformation into scattered amplitude. It can be rewritten

$$\frac{1}{2} A_c \underset{\sim}{\nabla} \cdot \underset{\sim}{v} = \frac{1}{2} \langle A_c \rangle \underset{\sim}{\nabla} \cdot \underset{\sim}{v} + \frac{1}{2} (A_c - \langle A_c \rangle) \underset{\sim}{\nabla} \cdot \underset{\sim}{v} . \qquad [17]$$

Taking the ensemble average of eq. 17, we have

$$\frac{1}{2} \langle A_c \underset{\sim}{\nabla} \cdot \underset{\sim}{v} \rangle = \frac{1}{2} \langle (A_c - \langle A_c \rangle) \underset{\sim}{\nabla} \cdot \underset{\sim}{v} \rangle . \qquad [18]$$

Whereas the function $(A_c - \langle A_c \rangle)$ is characterized by narrow negative spikes created by the shadows of the particles and does not depend at all on their refractive index, the random phase-front function $\underset{\sim}{\nabla} \cdot \underset{\sim}{v}$ is distributed more uniformly over the complete space and is a strong function of the refractive index of the particles. Therefore, $(A_c - \langle A_c \rangle)$ is, for all practical purposes, not correlated to $\underset{\sim}{\nabla} \cdot \underset{\sim}{v}$ and it follows from eq. 18 that

$$\frac{1}{2} \langle A_c \underset{\sim}{\nabla} \cdot \underset{\sim}{v} \rangle = 0 , \qquad [19]$$

and similarly that

$$\langle A_c \, w \rangle = 0 . \qquad [20]$$

Using eqs. 9-20 and applying them to both the forward and the backward fields, noting that $\langle A \rangle = \langle A_c \rangle$, dropping the subscript c when

not necessary, and taking the ensemble average (term by term) of the stochastic eqs. 5-8, we derive the following set of deterministic equations for the average wave front angles and wave amplitudes:

$$\frac{\partial \langle \underset{\sim}{V}_f \rangle}{\partial x} + \langle \underset{\sim}{V}_f \rangle \cdot \underset{\sim}{\nabla} \langle \underset{\sim}{V}_f \rangle = \underset{\sim}{\nabla} [\langle U \rangle - \langle \underset{\sim}{v}_f \cdot \underset{\sim}{v}_f \rangle], \qquad [21]$$

$$- \frac{\partial \langle \underset{\sim}{V}_b \rangle}{\partial x} + \langle \underset{\sim}{V}_b \rangle \cdot \underset{\sim}{\nabla} \langle \underset{\sim}{V}_b \rangle = \underset{\sim}{\nabla} [\langle U \rangle - \langle \underset{\sim}{v}_b \cdot \underset{\sim}{v}_b \rangle], \qquad [22]$$

$$\frac{\partial \langle A_f \rangle}{\partial x} + \langle \underset{\sim}{V}_f \rangle \cdot \underset{\sim}{\nabla} \langle A_f \rangle + \frac{1}{2} \langle A_f \rangle \underset{\sim}{\nabla} \cdot \langle \underset{\sim}{V}_f \rangle + k \langle W \rangle \langle A_f \rangle$$

$$- \frac{i}{2k} \nabla^2 \langle A_f \rangle = -k \langle w a_f \rangle - \underset{\sim}{\nabla} \cdot \langle \underset{\sim}{v}_f a_f \rangle + \frac{1}{2} \langle a_f \underset{\sim}{\nabla} \cdot \underset{\sim}{v}_f \rangle$$

$$+ \langle \tilde{S}_f e^{-ik(z + \phi_f)} \rangle, \qquad [23]$$

$$- \frac{\partial \langle A_b \rangle}{\partial x} + \langle \underset{\sim}{V}_b \rangle \cdot \underset{\sim}{\nabla} \langle A_b \rangle + \frac{1}{2} \langle A_b \rangle \underset{\sim}{\nabla} \cdot \langle \underset{\sim}{V}_b \rangle + k \langle W \rangle \langle A_b \rangle$$

$$- \frac{i}{2k} \nabla^2 \langle A_b \rangle = -k \langle w a_b \rangle - \underset{\sim}{\nabla} \cdot \langle \underset{\sim}{v}_b a_b \rangle + \frac{1}{2} \langle a_b \underset{\sim}{\nabla} \cdot \underset{\sim}{v}_b \rangle$$

$$+ \langle \tilde{S}_b e^{-ik(-z + \phi_b)} \rangle. \qquad [24]$$

Subtracting eqs. 23 and 24 from eqs. 7 and 8 respectively, and using eqs. 9-20, we arrive at the equations for the random amplitudes a_f and a_b,

$$\frac{\partial a_f}{\partial x} + \langle \underset{\sim}{V}_f \rangle \cdot \underset{\sim}{\nabla} a_f + \frac{1}{2} a_f \underset{\sim}{\nabla} \cdot \langle \underset{\sim}{V}_f \rangle + k \langle W \rangle a_f - \frac{i}{2k} \nabla^2 a_f$$

$$= - \{k w a_f - k \langle w a_f \rangle\} - k w A_{cf} - \frac{1}{2} A_{cf} \cdot \underset{\sim}{\nabla} \underset{\sim}{v}_f$$

$$- \{\underset{\sim}{v}_f \cdot \underset{\sim}{\nabla} a_f + \tfrac{1}{2} a_f \underset{\sim}{\nabla} \cdot \underset{\sim}{v}_f - \underset{\sim}{\nabla} \cdot \langle \underset{\sim}{v}_f a_f \rangle + \tfrac{1}{2} \langle a_f \underset{\sim}{\nabla} \cdot \underset{\sim}{v}_f \rangle\}$$

$$+ \{\tilde{S}_f \exp[-ik(z+\phi_f)] - \langle \tilde{S}_f \exp[-ik(z+\phi_f)] \rangle\}, \qquad [25]$$

$$- \frac{\partial a_b}{\partial z} + \langle \underset{\sim}{v}_b \rangle \cdot \underset{\sim}{\nabla} a_b + \tfrac{1}{2} a_b \underset{\sim}{\nabla} \cdot \langle \underset{\sim}{v}_b \rangle + k \langle w \rangle a_b - \frac{i}{2k} \nabla^2 a_b$$

$$= - \{kwa_b - k\langle wa_b \rangle\} - kwA_{cb} - \tfrac{1}{2} A_{cb} \cdot \underset{\sim}{\nabla} \underset{\sim}{v}_b$$

$$- \{\underset{\sim}{v}_b \cdot \underset{\sim}{\nabla} a_b + \tfrac{1}{2} a_b \underset{\sim}{\nabla} \cdot \underset{\sim}{v}_b - \underset{\sim}{\nabla} \cdot \langle \underset{\sim}{v}_b a_b \rangle + \tfrac{1}{2} \langle a_b \underset{\sim}{\nabla} \cdot \underset{\sim}{v}_b \rangle\}$$

$$+ \{\tilde{S}_b \exp[-ik(-z+\phi_b)] - \langle \tilde{S}_b \exp[-ik(-z+\phi_b)] \rangle\}. \qquad [26]$$

Finally, the equations for the average forward- and backward-scattered irradiance are readily obtained from eqs. 25-26 and 16-20. They are

$$\frac{\partial \langle a_f a_f^* \rangle}{\partial z} + \langle \underset{\sim}{v}_f \rangle \cdot \underset{\sim}{\nabla} \langle a_f a_f^* \rangle + \langle a_f a_f^* \rangle \underset{\sim}{\nabla} \cdot \langle \underset{\sim}{v}_f \rangle + 2k \langle w \rangle \langle a_f a_f^* \rangle$$

$$- \frac{i}{2k} \underset{\sim}{\nabla} \cdot [\langle a_f^* \underset{\sim}{\nabla} a_f \rangle - \langle a_f \underset{\sim}{\nabla} a_f^* \rangle]$$

$$= - 2k \langle wa_f a_f^* \rangle - k \langle wa_f \rangle \langle A_f \rangle^* - k \langle wa_f^* \rangle \langle A_f \rangle$$

$$- \tfrac{1}{2} \langle A_f \rangle \langle a_f^* \underset{\sim}{\nabla} \cdot \underset{\sim}{v}_f \rangle - \tfrac{1}{2} \langle A_f \rangle^* \langle a_f \underset{\sim}{\nabla} \cdot \underset{\sim}{v}_f \rangle$$

$$- \underset{\sim}{\nabla} \cdot \langle \underset{\sim}{v}_f a_f a_f^* \rangle + \langle a_f^* \tilde{S}_f \exp[-ik(z+\phi_f)] \rangle$$

$$+ \langle a_f \tilde{S}_f^* \exp[+ik(z+\phi_f)] \rangle, \qquad [27]$$

$$\frac{\partial \langle a_b a_b^* \rangle}{\partial z} + \langle \underset{\sim}{v}_b \rangle \cdot \underset{\sim}{\nabla} \langle a_b a_b^* \rangle + \langle a_b a_b^* \rangle \underset{\sim}{\nabla} \cdot \langle \underset{\sim}{v}_b \rangle + 2k \langle w \rangle \langle a_b a_b^* \rangle$$

$$- \frac{i}{2k} \underset{\sim}{\nabla} \left[\langle a_b^* \underset{\sim}{\nabla} a_b \rangle - \langle a_b \underset{\sim}{\nabla} a_b^* \rangle \right]$$

$$= - 2k \langle \omega_b a_b^* \rangle - k \langle \omega_b \rangle \langle A_b \rangle^* - k \langle \omega_b^* \rangle \langle A_b \rangle$$

$$- \frac{1}{2} \langle A_b \rangle \langle a_b^* \underset{\sim}{\nabla} \cdot \underset{\sim}{v}_b \rangle - \frac{1}{2} \langle A_b \rangle^* \langle a_b \underset{\sim}{\nabla} \cdot \underset{\sim}{v}_b \rangle$$

$$- \underset{\sim}{\nabla} \cdot \langle \underset{\sim}{v}_b a_b a_b^* \rangle + \langle a_b^* \tilde{S}_b \exp[-ik(-z+\phi_b)] \rangle$$

$$+ \langle a_b \tilde{S}_b^* \exp[+ik(-z+\phi_b)] \rangle. \qquad [28]$$

The system of deterministic eqs. 21-24 and 27-28 is mathematically unclosed insofar as it contains more unknowns than equations, such as the moments $\langle v_f a_f \rangle$, $\langle a_f \underset{\sim}{\nabla} \cdot \underset{\sim}{v}_f \rangle$, etc. This is the classic closure problem always encountered in the treatment of statistical phenomena governed by nonlinear and/or quasi-linear stochastic equations, such as eqs. 5-8. The complete mathematical model contains an infinite set of equations. Hence, workable models require closing this hierarchy of equations at a practical order.

The set of eqs. 21-24 and 27-28 is exact in the framework of unpolarized forward- and backward-propagating waves scattered by a particulate medium, but it is indeterminate. The essence of the proposed model will consist in deriving constitutive relations to relate the unknown statistical moments on the right-hand sides of eqs. 21-24 and 27-28 to the lower order functions $\langle A \rangle$ and $\langle aa^* \rangle$.

4.0 MODEL

4.1 Source-Sink Terms

The first element of the model is the formulation of the source-sink terms. These terms are responsible for the interchange of energy between the forward- and the backward-propagating waves. This interaction arises because of the backward reflection and scattering by the individual particles of a fraction of the impinging radiation. Instead of trying to solve this problem by rigourously applying the electromagnetic boundary conditions at the interface of the particles and the surrounding medium, we model the backscattering source-sink terms in a form mathematically similar to the forward scattering interaction as expressed by the terms of the form $\frac{1}{2}$ AV.$\underset{\sim}{V}$ of eq. 15. Hence, we write

$$\tilde{S}_f = \frac{1}{2} e^{ik(z+\phi_b)} A_b \underset{\sim}{V} \cdot (\underset{\sim}{v}_b^- - \underset{\sim}{v}_f^-), \qquad [29]$$

$$\tilde{S}_b = \frac{1}{2} e^{ik(-z+\phi_f)} A_f \underset{\sim}{V} \cdot (v_f^- - \underset{\sim}{v}_b^-), \qquad [30]$$

where $\underset{\sim}{v}_f^-$ and $\underset{\sim}{v}_b^-$ are the backscattered random geometric phase front angles of the forward and backward wave respectively. They will be determined by application of the reflection-refraction laws at the interface of the particles.

The mechanism of separation into a forward and a backward component modeled by eqs. 29 and 30 is somewhat arbitrary. The original Maxwell's equations contain no such distinction. In effect, eqs. 29 and 30 amount to a special and simplified treatment of the boundary conditions at the interface of the particles. Although heuristic, this separation into forward- and backscattering is very convenient in practical applications.

4.2 Hypotheses

The second most important element of the model is the derivation of the constitutive relations for the higher order unknown moments. The derivation is based on the following hypotheses:

Hypothesis 1. The random phase front angle $\underset{\sim}{\gamma}$ and amplitude a are only weakly correlated. This approximation is consistent with the governing eqs. 5-8, for they imply that $\underset{\sim}{\gamma}$ is independent of a and that the random a is the result of repeated interactions with the phase front angle $\underset{\sim}{\gamma}$ over the complete propagation path and not only at the point of observation. What the hypothesis means, for instance, is that

$$\langle \underset{\sim}{\gamma} a \rangle \ll \langle \underset{\sim}{\gamma}\,\underset{\sim}{\gamma} \rangle^{\frac{1}{2}} \langle a a^* \rangle^{\frac{1}{2}}. \qquad [31]$$

Such a relation was experimentally verified in the random continuous medium of turbulence (Ref. 18). In particulate media, we have no such direct measurements but the hypothesis is self-consistent. For example, the result obtained for $\langle \underset{\sim}{\gamma} a \rangle$ satisfies the inequality [31] if $\langle \underset{\sim}{\gamma} \cdot \underset{\sim}{\gamma} \rangle^{\frac{1}{2}} \ll 1$. From the equation for $\underset{\sim}{\gamma}$, we find that the standard deviation of $\underset{\sim}{\gamma}$, i.e. $\langle \underset{\sim}{\gamma} \cdot \underset{\sim}{\gamma} \rangle^{\frac{1}{2}}$, is of the order of the fraction of volume occupied by the particles to the power $\frac{1}{2}$. For naturally occurring aerosols, this quantity rarely exceeds 10^{-5} which gives $\langle \underset{\sim}{\gamma} \cdot \underset{\sim}{\gamma} \rangle^{\frac{1}{2}} \approx 0.06$. Hence, the results derived from Hypothesis 1 are self-consistent under most practical conditions.

Hypothesis 2. The cross correlations between quantities pertaining to the forward and backward waves are negligible, e.g.

$$\langle \underset{\sim}{\gamma}_b \cdot \underset{\sim}{\gamma}_f \rangle \approx \langle a_b\, a_f^* \rangle \approx 0. \qquad [32]$$

Although there is some interdependence between the forward and backward waves, the local quantities depend mostly on the random properties of statistically independent regions of the scattering medium. Hence, the hypothesis appears well justified, especially since the cross-correlation terms are always neglected by comparison with direct-correlation terms.

Hypothesis 3. Although not essential, we make the paraxial approximation. This considerably simplifies the mathematics and follows from our finding that the standard deviation of the random phase front angle is not larger than ~0.06 for most practical applications.

Hypothesis 4. The particulate medium is statistically homogeneous and isotropic over a domain the size of the beam diameter. This approximation is well justified for propagation of low-divergence laser beams.

Hypothesis 5. The random phase front angle is statistically homogeneous and isotropic in the plane transverse to the main direction of propagation, the 0-z axis. This is consistent with Hypotheses 3 and 4 which guarantee that all the rays reaching a plane z traverse statistically equivalent paths.

Hypothesis 6. The complex amplitude covariance function is quasi-homogeneous and quasi-isotropic in the transverse plane. More specifically, we assume that it is of the form

$$\langle a(z_1,\underset{\sim}{r}_1)a^*(z_2,\underset{\sim}{r}_2)\rangle = F[z_1,z_2;(\underset{\sim}{r}_1+\underset{\sim}{r}_2)/2]\cdot f[z_1,z_2;\ \underset{\sim}{r}_1-\underset{\sim}{r}_2], \quad [33]$$

where F and f are unspecified functions used to illustrate the functional dependence only. This is a standard approximation made in the presence of an average gradient. It is not essential but very convenient.

4.3 Constitutive Relations

From Hypotheses 3-5, eqs. 21 and 22 simplify to

$$\frac{\partial \langle \underset{\sim}{V}_f \rangle}{\partial z} + \langle \underset{\sim}{V}_f \rangle \cdot \underset{\sim}{\nabla}_\perp \langle \underset{\sim}{V}_f \rangle = 0, \qquad [34]$$

$$-\frac{\partial \langle \underset{\sim}{V}_b \rangle}{\partial z} + \langle \underset{\sim}{V}_b \rangle \cdot \underset{\sim}{\nabla}_\perp \langle \underset{\sim}{V}_b \rangle = 0, \qquad [35]$$

where $\underset{\sim}{\nabla}_\perp$ denotes the two-dimensional gradient operator in the transverse plane, i.e. with respect to the two-dimensional position vector $\underset{\sim}{r}$. Equations 34 and 35 show that the average phase front angle is independent of the statistical properties of the medium. The solution of eq. 34 for an initially spherical phase front with radius of curvature (focal distance) F is given by

$$\langle \underset{\sim}{V}_f \rangle = \underset{\sim}{r}/(z-F). \qquad [36]$$

From eq. 27 and the assumption of statistical symmetry of the scattering pattern with respect to the incident ray it follows that

$$\langle \underset{\sim}{V}_b \rangle = -\langle \underset{\sim}{V}_f \rangle = -\underset{\sim}{r}/(z-F). \qquad [37]$$

The first step toward the determination of the constitutive relations is the solution for the random amplitudes a_f and a_b. Solving implicitly eqs. 25 and 26 with the respective boundary conditions $a_f(z=0) = 0$ and $a_b(z=Z) = 0$, we find

$$a_f(z,\underset{\sim}{r}) = \frac{ik}{2\pi} \exp\left\{-\int_0^z k\langle W\rangle dz'\right\} \int_0^z \frac{dx}{x-z} \iint_{-\infty}^{\infty} d^2\underset{\sim}{s}\, g_f(x,\underset{\sim}{s})$$

$$\cdot \exp\left\{\frac{ik}{2(z-x)} \frac{F-z}{F-x} \left| \frac{F-x}{F-z}\, \underset{\sim}{r} - \underset{\sim}{s} \right|^2 + \int_0^x k\langle W\rangle dz'\right\}, \qquad [38]$$

$$a_b(z,\underset{\sim}{r}) = \frac{ik}{2\pi} \exp\left\{-\int_z^Z k\langle W\rangle dz'\right\} \int_z^Z \frac{dx}{z-x} \iint_{-\infty}^{\infty} d^2\underset{\sim}{s}\, g_b(x,\underset{\sim}{s})$$

$$\cdot \exp\left\{\frac{ik}{2(x-z)} \frac{z-F}{x-F} \left| \frac{x-F}{z-F} \underset{\sim}{r} - \underset{\sim}{s} \right|^2 + \int_x^Z k\langle W\rangle dz'\right\}, \quad [39]$$

where $g_f(x,\underset{\sim}{s})$ and $g_b(x,\underset{\sim}{s})$ stand for the right-hand sides of eqs. 25 and 26 respectively and where the solutions [36] and [37] have been substituted for $\langle \underset{\sim}{V}_f \rangle$ and $\langle \underset{\sim}{V}_b \rangle$. Equations 38 and 39 are implicit solutions for the forward and backward random amplitudes since the functions g_f and g_b contain a_f and a_b.

The unknown higher order moments are $\langle w a_f \rangle$, $\langle \underset{\sim}{v}_f a_f \rangle$, $\langle a_f \underset{\sim}{\nabla}_\perp \cdot \underset{\sim}{v}_f \rangle$, etc. The procedure to relate these moments to the lower order $\langle A \rangle$ and/or $\langle aa^* \rangle$ is basically the same for all of them. The implicit solution for a_f (or a_b) is first multiplied by w, or $\underset{\sim}{v}_f$, or $\underset{\sim}{\nabla} \cdot \underset{\sim}{v}_f$, etc..., and the products are then ensemble averaged. This produces many terms under the integral operator of eq. 38 or 39. Most of them can be neglected in relation to a leading term on account of Hypothesis 1, and further mathematical simplifications can be worked out using Hypotheses 2-6. These derivation steps are lengthy and will not be repeated here; however they are similar to those followed in Refs. 19 and 20. The resulting constitutive closure relations are

$$k \langle w a_f \rangle \approx -\frac{1}{2} \sigma_{af} \langle A_f \rangle, \quad [40]$$

$$k \langle w a_b \rangle \approx -\frac{1}{2} \sigma_{ab} \langle A_b \rangle, \quad [41]$$

$$k \langle w a_f a_f^* \rangle \approx -\frac{1}{2} \mathrm{Re}\,[\sigma_{afs}] \langle a_f a_f^* \rangle, \quad [42]$$

$$k \langle w a_b a_b^* \rangle \approx -\frac{1}{2} \mathrm{Re}\,[\sigma_{abs}] \langle a_b a_b^* \rangle, \quad [43]$$

$$\langle a_f \underset{\sim}{\nabla}_\perp \cdot \underset{\sim}{v}_f \rangle = - \sigma_{cf} \langle A_f \rangle, \qquad [44]$$

$$\langle a_b \underset{\sim}{\nabla}_\perp \cdot \underset{\sim}{v}_b \rangle = - \sigma_{cb} \langle A_b \rangle, \qquad [45]$$

$$\langle e^{ik(\phi_b - \phi_f)} a_b \underset{\sim}{\nabla}_\perp \cdot (\underset{\sim}{v}_b^- - \underset{\sim}{v}_f^-) \rangle = - \sigma_{cf}^- \langle A_f \rangle, \qquad [46]$$

$$\langle e^{ik(\phi_f - \phi_b)} a_f \underset{\sim}{\nabla}_\perp \cdot (\underset{\sim}{v}_f^- - \underset{\sim}{v}_b^-) \rangle = - \sigma_{cb}^- \langle A_b \rangle, \qquad [47]$$

$$\langle e^{ik(\phi_b - \phi_f)} a_f^* a_b \underset{\sim}{\nabla}_\perp \cdot (\underset{\sim}{v}_b^- - \underset{\sim}{v}_f^-) \rangle + \text{c.c.}$$

$$= 2\,\mathrm{Re}[\sigma_{sb}^-] \langle a_b a_b^* \rangle - 2\,\mathrm{Re}[\sigma_{sf}^-] \langle a_f a_f^* \rangle, \qquad [48]$$

$$\langle \underset{\sim}{v}_f a_f \rangle = 0, \qquad [49]$$

$$\langle \underset{\sim}{v}_b a_b \rangle = 0, \qquad [50]$$

$$\langle \underset{\sim}{v}_f a_f a_f^* \rangle = - \mathrm{Re}[\underset{\sim}{D}_f] \cdot \underset{\sim}{\nabla}_\perp \langle a_f a_f^* \rangle, \qquad [51]$$

$$\langle \underset{\sim}{v}_b a_b a_b^* \rangle = - \mathrm{Re}[\underset{\sim}{D}_b] \cdot \underset{\sim}{\nabla}_\perp \langle a_b a_b^* \rangle, \qquad [52]$$

where c.c. stands for the complex conjugate of the preceding term and where the quantities underlined by a double tilde are two-dimensional tensors or dyadics.

There are several constitutive relations but they can all be classified in one of three categories: the particle absorption terms, eqs. 40-43; the aerosol forward- and backscattering terms, eqs. 44-48; and the diffusion terms, eqs. 49-52.

The coefficients of eqs. 40-52 are given by the integral operator 38 or 39 operating on various covariance functions. To simplify the algebra, we restrict applications to slightly diverging beams. In that case, the focal length F of eqs. 38 and 39 is large and negative.

Moreover, the covariance functions operated upon have longitudinal correlation lengths that are generally much smaller than $|F-z|$ and thus the major contributions to the integrals come from values of x in the immediate neighbourhood of z compared with $|F-z|$. Hence, we can make the approximation

$$\frac{F-z}{F-x} \approx 1, \qquad [53]$$

and the following simplified operators 0^+ and 0^- can be written from eqs. 38 and 39:

$$0^+\{h(z,\underset{\sim}{r};\eta,\rho)\} = -\frac{ki}{2\pi}\int_0^z \frac{d\eta}{\eta} e^{-\Delta_f(z,\eta)} \iint_{-\infty}^{\infty} d^2\rho\, e^{\frac{ik\rho^2}{2\eta}} h(z,\underset{\sim}{r};\eta,\rho), \qquad [54]$$

$$0^-\{h(z,\underset{\sim}{r};\eta,\rho)\} = -\frac{ki}{2\pi}\int_0^{Z-z} \frac{d\eta}{\eta} e^{-\Delta_b(z,\eta)} \iint_{-\infty}^{\infty} d^2\rho\, e^{\frac{ik\rho^2}{2\eta}} h(z,\underset{\sim}{r};\eta,\rho), \qquad [55]$$

where $h(z,\underset{\sim}{r};\eta,\rho)$ is a dummy function and where

$$\Delta_f(z,\eta) = \int_0^{\eta} k\langle W(z-x')\rangle\, dx', \qquad [56]$$

$$\Delta_b(z,\eta) = \int_0^{\eta} k\langle W(z-x')\rangle\, dx'. \qquad [57]$$

In terms of the operators 0^+ and 0^-, the particle absorption coefficients are given by

$$\sigma_{af} = 2k^2\, 0^+\{\langle w(1)w(2)\rangle\}, \qquad [58]$$

$$\sigma_{ab} = 2k^2\, 0^-\{\langle w(1)w(2)\rangle\}, \qquad [59]$$

$$\sigma_{afs} = 2k^2\, 0^+\{G_f(z,\eta,\rho)\ \langle w(1)w(2)\rangle\}, \qquad [60]$$

$$\sigma_{abs} = 2k^2\, 0^- \{G_b(z,\eta,\rho)\ \langle w(1)\, w(2)\rangle\}, \qquad [61]$$

the scattering coefficients by

$$\sigma_{cf} = -\tfrac{1}{2}\, 0^+ \{\underset{\sim}{\nabla}_\rho\, \underset{\sim}{\nabla}_\rho : \langle \underset{\sim}{v}_f(1)\, \underset{\sim}{v}_f(2)\rangle\}, \qquad [62]$$

$$\sigma_{cb} = -\tfrac{1}{2}\, 0^- \{\underset{\sim}{\nabla}_\rho\, \underset{\sim}{\nabla}_\rho : \langle \underset{\sim}{v}_b(1)\, \underset{\sim}{v}_b(2)\rangle\}, \qquad [63]$$

$$\bar{\sigma}_{cf} = -\tfrac{1}{2}\, 0^- \{H(z,\eta,\rho)\ \underset{\sim}{\nabla}_\rho\, \underset{\sim}{\nabla}_\rho : [\langle \underset{\sim}{v}_f^-(1)\, \underset{\sim}{v}_f^-(2)\rangle + \langle \underset{\sim}{v}_b^-(1)\, \underset{\sim}{v}_b^-(2)\rangle]\}, \qquad [64]$$

$$\bar{\sigma}_{cb} = -\tfrac{1}{2}\, 0^+ \{H(z,\eta,\rho)\ \underset{\sim}{\nabla}_\rho\, \underset{\sim}{\nabla}_\rho : [\langle \underset{\sim}{v}_f^-(1)\, \underset{\sim}{v}_f^-(2)\rangle + \langle \underset{\sim}{v}_b^-(1)\, \underset{\sim}{v}_b^-(2)\rangle]\}, \qquad [65]$$

$$\bar{\sigma}_{sf} = -\tfrac{1}{2}\, 0^- \{H(z,\eta,\rho)\ G_f(z,\eta,\rho)\ \underset{\sim}{\nabla}_\rho\, \underset{\sim}{\nabla}_\rho : [\langle \underset{\sim}{v}_f^-(1)\, \underset{\sim}{v}_f^-(2)\rangle + \langle \underset{\sim}{v}_b^-(1)\, \underset{\sim}{v}_b^-(2)\rangle]\}, \qquad [66]$$

$$\bar{\sigma}_{sb} = -\tfrac{1}{2}\, 0^+ \{H(z,\eta,\rho)\ G_b(z,\eta,\rho)\ \underset{\sim}{\nabla}_\rho\, \underset{\sim}{\nabla}_\rho : [\langle \underset{\sim}{v}_f^-(1)\, \underset{\sim}{v}_f^-(2)\rangle + \langle \underset{\sim}{v}_b^-(1)\, \underset{\sim}{v}_b^-(2)\rangle]\}, \qquad [67]$$

and the diffusion coefficients by

$$\underset{\sim}{D}_f = \tfrac{1}{2}\, 0^+ \{G_f(z,\eta,\rho)\ \langle \underset{\sim}{v}_f(1)\, \underset{\sim}{v}_f(2)\rangle\}, \qquad [68]$$

$$\underset{\sim}{D}_b = \tfrac{1}{2}\, 0^- \{G_b(z,\eta,\rho)\ \langle \underset{\sim}{v}_b(1)\, \underset{\sim}{v}_b(2)\rangle\}, \qquad [69]$$

where (1) and (2) refer to the adjacent points $(z, \underset{\sim}{r}+\rho/2)$ and $(z-\eta, \underset{\sim}{r}-\rho/2)$ of the covariance functions and where

$$G_f(z,\eta,\rho) = \langle a_f(1)\, a_f^*(2)\rangle \,/\, \langle a_f a_f^*\rangle, \qquad [70]$$

$$G_b(z,\eta,\rho) = \langle a_b(1)\, a_b^*(2)\rangle \,/\, \langle a_b a_b^*\rangle, \qquad [71]$$

$$H(z,\eta,\rho) = \langle e^{ik[\phi_b(1)-\phi_b(2)-\phi_f(1)+\phi_f(2)]}\rangle. \qquad [72]$$

The list of symbols at the beginning of this report defines the individual absorption, scattering and diffusion coefficients.

4.4 Propagation Coefficients

The absorption coefficients σ_{af} and σ_{ab} depend on the covariance function $\langle w(1)\, w(2)\rangle$ which involves the real and imaginary parts of the random refractive index as defined by eqs. 10 and 12. $\langle w(1)\, w(2)\rangle$ can be determined from the specified medium and particle properties, i.e. the complex refractive indices of the medium and the particles, the shape of the particles, their number density, and their size distribution. Then, σ_{af} and σ_{ab} can be calculated by direct substitution in eqs. 58 and 59. Because of Hypothesis 4, the covariance function $\langle w(1)\, w(2)\rangle$ is independent of $\underset{\sim}{r}$ over a domain the size of the beam diameter. Hence, the coefficients σ_{af} and σ_{ab} are functions of the longitudinal coordinate z only. These coefficients are second-order corrections to the absorption coefficient $k\langle W\rangle$ of eqs. 23-24 and 27-28.

There are two additional absorption coefficients σ_{afs} and σ_{abs} which depend on the amplitude correlation functions G_f and G_b. The latter functions are not known but their correlation lengths are expected to be much greater than that of $\langle w(1)\, w(2)\rangle$ equal to the average particle size. Hence, both G_f and G_b may be replaced (in eqs. 60 and 67) by their values at the origin which, by definition, are equal to unity. Therefore, the coefficients σ_{afs} and σ_{abs} are respectively equal to σ_{af} and σ_{ab}.

The calculation of the scattering coefficients (eqs. 62-67) and the diffusion coefficients (eqs. 68-69) requires knowledge of the phase front angle covariance functions. These cannot be inferred directly from the medium and particle properties but only through the solution of the ray propagation equation. The procedure is to derive the equations for the covariances of $\underset{\sim}{v}_f$ and $\underset{\sim}{v}_b$ from eqs. 5, 6, 21 and 22. The result for slightly diverging beam waves and approximately Gaussian statistics for $\underset{\sim}{v}_f$ and $\underset{\sim}{v}_b$ is

$$\frac{\partial^2}{\partial x^2} \langle \underset{\sim}{v}_f(1)\, \underset{\sim}{v}_f(2) \rangle - \frac{\partial^2}{\partial \eta^2} \langle \underset{\sim}{v}_f(1)\, \underset{\sim}{v}_f(2) \rangle - \frac{1}{2} \underset{\sim}{\nabla}_\rho\, \underset{\sim}{\nabla}_\rho \left[\langle \underset{\sim}{v}_f(1)\, \underset{\sim}{v}_f(2) \rangle : \right.$$

$$\left. \langle \underset{\sim}{v}_f(1)\, \underset{\sim}{v}_f(2) \rangle \right] = -\frac{1}{4} \underset{\sim}{\nabla}_\rho\, \underset{\sim}{\nabla}_\rho \langle u(1)\, u(2) \rangle, \qquad [73]$$

and a similar equation for $\langle \underset{\sim}{v}_b(1)\, \underset{\sim}{v}_b(2) \rangle$. The source term $\langle u(1)\, u(2) \rangle$ on the right-hand side of eq. 73 can be determined from the properties of the particulate medium in the same fashion as for the function $\langle w(1)\, w(2) \rangle$ discussed earlier. Therefore, the solution for $\langle \underset{\sim}{v}_f(1)\, \underset{\sim}{v}_f(2) \rangle$ can in principle be worked out from eq. 73, and similarly for $\langle \underset{\sim}{v}_b(1)\, \underset{\sim}{v}_b(2) \rangle$.

The solution of eq. 73 cannot be treated exactly because of the nonlinear term. No satisfactory method of solution has been derived yet. However, a preliminary analysis was carried out and order-of-magnitude estimates were derived. Since the analysis is incomplete and may have to be reexamined, only the results will be presented here.

First, the covariance function $\langle \underset{\sim}{v}_f(1)\, \underset{\sim}{v}_f(2) \rangle$ scales as

$$\langle \underset{\sim}{v}_f \cdot \underset{\sim}{v}_f \rangle = O(\langle u^2 \rangle^{\frac{1}{2}}). \qquad [74]$$

For naturally occurring fogs, we obtain from eq. 74 that the standard deviation of the forward phase front angle fluctuations is of the order

of 10 mrad, in qualitative agreement with observations. Second, the longitudinal correlation length of $\langle \underset{\sim}{v}_f(1)\ \underset{\sim}{v}_f(2)\rangle$ is

$$L = \frac{1}{v\pi\langle b^2\rangle}, \qquad [75]$$

where v is the particles number density and $\pi\langle b^2\rangle$ is the average particle cross section. Finally, the transverse correlation scale is

$$\ell = \langle \underset{\sim}{v}_f \cdot \underset{\sim}{v}_f\rangle^{\frac{1}{2}} L, \qquad [76]$$

which is generally much greater than the average particle radius $\langle b\rangle$ characterizing the index covariance function $\langle u(1)\ u(2)\rangle$. Therefore, in addition to the nonlinearity, analysis of eq. 73 is further complicated by the presence of the three disparate scales L, ℓ, and $\langle b\rangle$. This is particularly troublesome in setting up finite difference methods of solution. The results are similar for $\langle \underset{\sim}{v}_b(1)\ \underset{\sim}{v}_b(2)\rangle$.

Because of the presence of the derivatives with respect to z in eq. 73, the quantities $\langle \underset{\sim}{v}_f \cdot \underset{\sim}{v}_f\rangle$, L, and ℓ are not truly local properties but they include some form of history of the medium through which the wave has propagated. In particular, there exists a transition region near the boundaries of the scattering medium. The size of the dispersion domain varies with the local conditions and is of the order of $L \times \ell$.

For the backscattering coefficients, we need the functions $\langle \underset{\sim}{v}_f^-(1)\ \underset{\sim}{v}_f^-(2)\rangle$ and $\langle \underset{\sim}{v}_b^-(1)\ \underset{\sim}{v}_b^-(2)\rangle$. These are somewhat easier to determine because they are not propagated. They define the backscattering properties at the location where the backscattering occurs. Since the scatterers are statistically independent, the correlation does not extend very far. Transversely, the functions $\langle \underset{\sim}{v}_f^-(1)\ \underset{\sim}{v}_f^-(2)\rangle$ and $\langle \underset{\sim}{v}_b^-(1)\ \underset{\sim}{v}_b^-(2)\rangle$ correlate over a region of the same size as the particles, i.e.

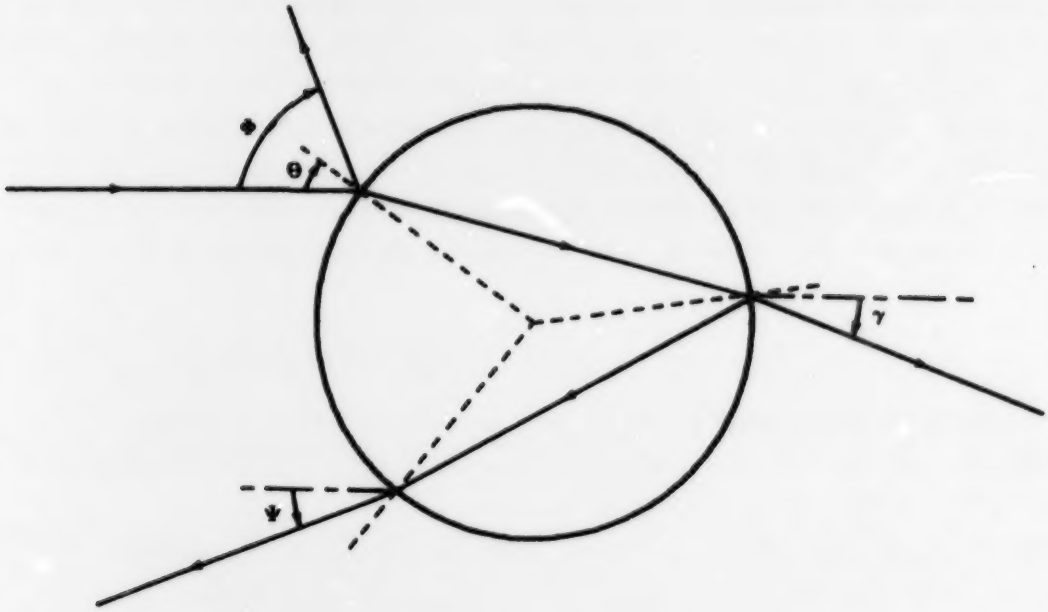

FIGURE 1 - Diagram of primary reflected and refracted optical rays in the plane of incidence on a spherical particle of index n surrounded by a medium of index 1.

$$\bar{\ell} = \langle b \rangle. \qquad [77]$$

The contributions measured at points more widely separated are uncorrelated because they originate from different and uncoupled particles. Longitudinally, the average thickness of the scattering sheet over which there is coherence is approximated by the mean distance between the particles, i.e.

$$\bar{L} = \left(\frac{3}{4\pi\nu}\right)^{1/3}. \qquad [78]$$

The variances $\langle \bar{v}_{\sim f} \cdot \bar{v}_{\sim f} \rangle$ and $\langle \bar{v}_{\sim b} \cdot \bar{v}_{\sim b} \rangle$ are inferred from the propagated $\langle v_{\sim f} \cdot v_{\sim f} \rangle$ and $\langle v_{\sim b} \cdot v_{\sim b} \rangle$ by applying the refraction-reflection boundary conditions at the interface between the particles and the

surrounding medium. Figure 1 illustrates the situation for the special case of spherical particles. There are two principal contributions characterized by one external reflection and by one refraction followed by one internal reflection, respectively. The incidence and exit angles defined in Fig. 1 are related as follows

$$\phi = 2\,\theta, \qquad [79]$$

$$\phi = 2\,\theta - 2\,\gamma, \qquad [80]$$

where

$$\sin\gamma = \frac{2}{n_p^2}\sin\theta\cos\theta\left[n_p^2 - 2\sin^2\theta\right] - \frac{2}{n_p^2}\sin\theta\sqrt{n_p^2 - \sin^2\theta}\left[1 - 2\sin^2\theta\right], \qquad [81]$$

and where n_p is the real part of the particle refractive index. The two main components of $\langle \underset{\sim}{v}_f^- \cdot \underset{\sim}{v}_f^- \rangle$ (or $\langle \underset{\sim}{v}_b^- \cdot \underset{\sim}{v}_b^- \rangle$) for a single particle are proportional to the variances $\langle\phi^2\rangle$ and $\langle\Psi^2\rangle$ calculated over the forward scattering angle γ. Since the scattering angle standard deviation is small, we assume that γ is distributed in such a way that the major contributions to $\langle\phi^2\rangle$ and $\langle\Psi^2\rangle$ come from small values of γ, which allows the linearization of eq. 81. Moreover, to model the average backscattering effects of the particles, we multiply $\langle\phi^2\rangle$ and $\langle\Psi^2\rangle$ by the reflection coefficient and by the fractional cross-sectional area of the particles over the scattering sheet of thickness L^-. We thus obtain

$$\langle \underset{\sim}{v}_f^- \cdot \underset{\sim}{v}_f^- \rangle_1 = \langle \underset{\sim}{v}_f \cdot \underset{\sim}{v}_f \rangle \frac{n_p^2}{(n_p+1)^2}\,\nu^{2/3}\langle b^2\rangle, \qquad [82]$$

$$\langle \underset{\sim}{v}_f^- \cdot \underset{\sim}{v}_f^- \rangle_2 \approx \langle \underset{\sim}{v}_f \cdot \underset{\sim}{v}_f \rangle \frac{16 n_p^2 (2-n_p)^2}{(n_p+1)^2} \nu^{2/3} \langle b^2 \rangle, \quad [83]$$

$$\langle \underset{\sim}{v}_b^- \cdot \underset{\sim}{v}_b^- \rangle_1 \approx \langle \underset{\sim}{v}_b \cdot \underset{\sim}{v}_b \rangle \frac{n_p^2}{(n_p+1)^2} \nu^{2/3} \langle b^2 \rangle, \quad [84]$$

$$\langle \underset{\sim}{v}_b^- \cdot \underset{\sim}{v}_b^- \rangle_2 \approx \langle \underset{\sim}{v}_b \cdot \underset{\sim}{v}_b \rangle \frac{16 n_p^2 (2-n_p)^2}{(n_p+1)^2} \nu^{2/3} \langle b^2 \rangle. \quad [85]$$

Equations 77, 78 and 82-85 constitute an order-of-magnitude representation of the covariance functions $\langle \underset{\sim}{v}_f^-(1)\ \underset{\sim}{v}_f^-(2) \rangle$ and $\langle \underset{\sim}{v}_b^-(1)\ \underset{\sim}{v}_b^-(2) \rangle$.

Some of the backscattering coefficients depend on the correlation function $H(z, \eta, \underset{\sim}{\rho})$ defined by eq. 72. Assuming Gaussian statistics for the random phase front fluctuations ϕ_f and ϕ_b, which is a justified standard approximation, we obtain from eq. 72

$$H(z, \eta, \underset{\sim}{\rho}) = e^{\frac{-k^2}{2}(P_f + P_b)}, \quad [86]$$

where P_f and P_b are the forward and backward phase structure functions. For optical and infrared waves, the wave number k is very large and eq. 86 can be satisfactorily approximated by the first term of the series expansions of P_f and P_b for small separation distances. These can be derived from the solutions for $\langle \underset{\sim}{v}_f(1)\ \underset{\sim}{v}_f(2) \rangle$. We thus obtain the following transverse and longitudinal correlation scales for $H(z, \eta, \underset{\sim}{\rho})$:

$$\ell_H = \frac{\lambda}{[\nu \langle a^3 \rangle]^{\frac{1}{2}}}, \quad [87]$$

$$L_H = \frac{\lambda}{[\nu \langle a^3 \rangle]^{\frac{1}{2}}}, \quad [88]$$

where λ is the wavelength. The scales ℓ_p and L_p are small but, for most practical applications, they remain much greater than the respective scales ℓ^- and L^- of $\langle \underset{\sim}{v}_f^-(1)\ \underset{\sim}{v}_f^-(2)\rangle$ and $\langle \underset{\sim}{v}_b^-(1)\ \underset{\sim}{v}_b^-(2)\rangle$. Therefore, we may set

$$H(x, \eta, \underset{\sim}{\rho}) \approx 1 \qquad [89]$$

in eqs. 64-67 with negligible consequences for the accuracy of the backscattering coefficients.

The scattering and diffusion coefficients also depend on the amplitude correlation functions G_f and G_b defined in eqs. 70 and 71. For the coefficients given by eqs. 60, 61, 66 and 67, the effects of G_f and G_b are negligible since the scale $\langle b\rangle$ of the covariance function $\langle w(1)\ w(2)\rangle$ and the scales ℓ^- and L^- of $\langle \underset{\sim}{v}_f^-(1)\ \underset{\sim}{v}_f^-(2)\rangle$ and $\langle \underset{\sim}{v}_b^-(1)\ \underset{\sim}{v}_b^-(2)\rangle$ are much smaller than the scales of either G_f and G_b. Consequently, the integrals can be calculated with good accuracy by substituting for G_f and G_b their values at the origin which, by definition, are equal to unity. However, in eqs. 68 and 69, the scales of G_f and G_b are comparable to those of the phase front covariance functions. But, even in these cases, the major contributions to the integrals come from the neighbourhood of the origin in the $(\eta, \underset{\sim}{\rho})$-space because of the effect of the rapidly oscillating term $\frac{1}{\eta} \exp\left[\frac{ik\rho^2}{2\eta}\right]$. Nevertheless, the complete formal treatment of the diffusion coefficients $\underset{\sim}{D}_f$ and $\underset{\sim}{D}_b$ requires the solution of G_f and G_b. Equations for G_f and G_b could be derived from the stochastic eqs. 5-8 but this would produce multidimensional differential equations and more unknown moments for which additional constitutive relations would have to be established. Instead, it is hoped that the following solutions, derived by neglecting diffraction, are sufficiently accurate to account for G_f and G_b in the region adjacent to the origin:

$$G_f(z,\eta,\rho) = \exp\left\{-\frac{1}{8}\int_0^{z+\eta/2}dz'\int_0^{z+\eta/2}dz''\lim_{\rho\to 0}\nabla_{\underset{\sim}{\rho}}\nabla_{\underset{\sim}{\rho}}:\langle \underset{\sim}{v}_f(z',\underset{\sim}{r}+\underset{\sim}{\rho}/2)\,\underset{\sim}{v}_f(z'',\underset{\sim}{r}-\underset{\sim}{\rho}/2)\rangle\right.$$

$$-\frac{1}{8}\int_0^{z-\eta/2}dz'\int_0^{z-\eta/2}dz''\lim_{\rho\to 0}\nabla_{\underset{\sim}{\rho}}\nabla_{\underset{\sim}{\rho}}:\langle \underset{\sim}{v}_f(z',\underset{\sim}{r}+\underset{\sim}{\rho}/2)\,\underset{\sim}{v}_f(z'',\underset{\sim}{r}-\underset{\sim}{\rho}/2)\rangle$$

$$-\frac{1}{8}\int_0^{z+\eta/2}dz'\int_0^{z-\eta/2}dz''\lim_{\rho\to 0}\nabla_{\underset{\sim}{\rho}}\nabla_{\underset{\sim}{\rho}}:\langle \underset{\sim}{v}_f(z',\underset{\sim}{r}+\underset{\sim}{\rho}/2)\,\underset{\sim}{v}_f(z'',\underset{\sim}{r}-\underset{\sim}{\rho}/2)\rangle$$

$$-\frac{1}{8}\int_0^{z-\eta/2}dz'\int_0^{z+\eta/2}dz''\lim_{\rho\to 0}\nabla_{\underset{\sim}{\rho}}\nabla_{\underset{\sim}{\rho}}:\langle \underset{\sim}{v}_f(z',\underset{\sim}{r}+\underset{\sim}{\rho}/2)\,\underset{\sim}{v}_f(z'',\underset{\sim}{r}-\underset{\sim}{\rho}/2)\rangle$$

$$\left.+\frac{1}{2}\int_0^{z}dz'\int_0^{z}dz''\lim_{\rho\to 0}\nabla_{\underset{\sim}{\rho}}\nabla_{\underset{\sim}{\rho}}:\langle \underset{\sim}{v}_f(z',\underset{\sim}{r}+\underset{\sim}{\rho}/2)\,\underset{\sim}{v}_f(z'',\underset{\sim}{r}-\underset{\sim}{\rho}/2)\rangle\right\}, \qquad [90]$$

and a similar equation for $G_b(z,\eta,\rho)$. This will have to be verified experimentally but the errors are expected to be small since the principal contribution to the integrals of eqs. 68 and 69 which come from the neighbourhood of the origin are independent of the approximation. The alternative is a much higher level of mathematical complexity or the need for some empirical input.

Equations 62-69 and 89-90 give the propagation coefficients in terms of the forward and backward phase front covariance functions. These functions satisfy nonlinear partial differential equations which were not solved in this report. The principal difficulties are the nonlinearity of the equations and the presence of three disparate scales: the average particle size, the mean distance between wave interactions with the particles, and the latter multiplied by the forward scattering phase front angle standard deviation. What was achieved in this report is the determination of these scales and the derivation of order-of-magnitude estimates of the pertinent variances.

Consequently, the present state of the model allows only rough estimates for the propagation coefficients.

Although a satisfactory solution of the nonlinear eq. 73 has yet to be derived, eqs. 58-69 together with eq. 73 for the phase front angle covariance function provide a formal framework for relating the propagation coefficients to the medium properties. Moreover, if eq. 90 holds, this problem is totally uncoupled from the propagation problem since the wave amplitude is not in eqs. 58-69. Therefore, the determination of the scattering and diffusion coefficients is a well-posed problem, albeit difficult, that can be handled independently of propagation. The situation is somewhat similar to the more common approach where Mie calculations, needed to specify the phase function, are performed independently of the solution of the radiative transfer equation.

Equations 58-69 are valid for inhomogeneous media, the only restriction being that the size of the inhomogeneities must be larger than the beam diameter. It must also be noted that the various scattering and diffusion coefficients are not truly local values. They bear some history of the scattering medium over a region defined by the convolution of the coherence domain of the phase front angle covariance functions with the integral operators 0^+ and 0^-.

The physical interpretations are straightforward. The scattering coefficients are responsible for the transfer of energy from the coherent state into the incoherent or scattered state, and from the forward propagating beam into the backward propagating beam and vice versa. The diffusion coefficients measure the rate at which the scattered energy is spatially diffused, or the rate at which the scattered beam spreads out. They account for the multiple scatterings.

The diffusion coefficients are dyadics or second-order tensors but all the components are not independent. From Hypothesis 5, the

phase front angle covariance functions are statistically homogeneous and isotropic in the plane normal to the propagation axis. The general form for such an isotropic tensor is (Ref. 21)

$$\langle \underset{\sim}{v}(1)\underset{\sim}{v}(2)\rangle = M(z,\eta,\rho^2)\ \underset{\sim}{\rho\rho} + N(z,\eta,\rho^2)\ \underset{\sim}{\delta}, \qquad [91]$$

where $\underset{\sim}{\delta}$ is the two-dimensional unit dyad or the two-dimensional Kronecker delta and M and N are scalar functions. The diffusion coefficients are thus given by an expression of the form

$$-\frac{ki}{2\pi}\int_0^z \frac{d\eta}{\eta}\, e^{-\Delta_f(z,\eta)} \iint_{-\infty}^{\infty} d^2\underset{\sim}{\rho}\ e^{\frac{ik\rho^2}{\eta}} \left[M(z,\eta,\rho^2)\underset{\sim}{\rho\rho} + N(z,\eta,\rho^2)\ \underset{\sim}{\delta}\right]$$

$$= -\frac{ki}{2}\int_0^z \frac{d\eta}{\eta}\, e^{-\Delta_f(z,\eta)} \int_0^{\infty} \rho d\rho\ e^{\frac{ik\rho^2}{2\eta}} \left[M(z,\eta,\rho^2)+2N(z,\eta,\rho^2)\right] \underset{\sim}{\delta}, \qquad [92]$$

or in shorter notation by

$$\underset{\sim}{D} = D\underset{\sim}{\delta}, \qquad [93]$$

where D is a scalar function of position z along the direction of propagation.

The mathematical difficulty of solving exactly for the scattering and diffusion coefficients will be dealt with in a subsequent work. In this report, we will proceed with the solution of the propagation equations. Comparison with experimental data or empirical modeling can always be used to determine the coefficients.

5.0 PROPAGATION EQUATIONS

The governing propagation equations are obtained by substituting the constitutive relations, eqs. 40-52, for the higher order unknown moments in eqs. 23, 24, 27 and 28. We limit the present analysis to the more practical case where there is only one coherent beam transmitted in what is chosen as the forward direction. Under this condition $\langle A_b \rangle = 0$. Moreover, we assume that the aerosol diffusion effect is much more important than the diffraction spreading of the beam, which is well justified in most applications. We can thus neglect the terms of the form $\frac{i}{2k} \underset{\sim}{\nabla}_\perp \cdot [\langle a^* \underset{\sim}{\nabla}_\perp a \rangle - \langle a \underset{\sim}{\nabla}_\perp a^* \rangle]$. With these approximations and using eqs. 36 and 37, we obtain the following set of propagation equations:

a) for the average reduced amplitude $A_r = \langle A_f \rangle$:

$$\frac{\partial A_r}{\partial z} + \frac{r}{z-F}\frac{\partial A_r}{\partial r} + \frac{A_r}{z-F} + \frac{1}{2}\left[\sigma_a - \sigma_{af} + \sigma_{cf} + \bar{\sigma}_{cf}\right]A_r - \frac{i}{2k}\nabla_\perp^2 A_r = 0, \quad [94]$$

b) for the forward-scattered irradiance $I^+ = \langle a_f a_f^* \rangle$:

$$\frac{\partial I^+}{\partial z} + \frac{r}{z-F}\frac{\partial I^+}{\partial r} + \frac{2I^+}{z-F} + \left[\sigma_a - \mathrm{Re}(\sigma_{afs}) + \mathrm{Re}(\bar{\sigma}_{sf})\right]I^+ - \mathrm{Re}(D_f)\nabla_\perp^2 I^+$$

$$= \mathrm{Re}(\sigma_{af} + \sigma_{cf})\, A_r A_r^* + \mathrm{Re}(\bar{\sigma}_{sb})I^-, \quad [95]$$

c) for the backscattered irradiance $I^- = \langle a_b a_b^* \rangle$

$$-\frac{\partial I^-}{\partial z} - \frac{r}{z-F}\frac{\partial I^-}{\partial r} - \frac{2I^-}{z-F} + \left[\sigma_a - \mathrm{Re}(\sigma_{abs}) + \mathrm{Re}(\bar{\sigma}_{sb})\right]I^- - \mathrm{Re}(D_b)\nabla_\perp^2 I^-$$

$$= R_e(\bar{\sigma}_{cf})\, A_r A_r^* + R_e(\bar{\sigma}_{sf})I^+, \quad [96]$$

where σ_a is the main contribution to the particle absorption coefficient defined by

$$\sigma_a = 2k\langle W\rangle. \qquad [97]$$

Equations 94-96 constitute the proposed propagation model. They form a closed set of three-dimensional, coupled, partial differential equations for the solution of the forward- and backscattered irradiance beam profiles resulting from a coherent optical or infrared beam directed into a particulate medium. The dimensions are reduced to two under cylindrical symmetry.

The various absorption, scattering and diffusion coefficients are formally related to the medium properties through eqs. 58-69. Homogeneity is assumed only on the scale of the beam diameter. The model handles all orders of scattering in a global fashion but cannot differentiate between them. However, the single-scattering results can be derived by dropping eqs. 95 and 96 and solving eq. 94. Similarly, the first-order multiple-scattering approximation for the backscattered beam can be modeled by setting $I^+ = 0$ in the right-hand side of eq. 96, and by arbitrarily adding the forward-scattering coefficient $R_e(\sigma_{cf})$ to $[\sigma_a - Re(\sigma_{abs}) + Re(\sigma_{sb}^-)]$ in the left-hand side of the same equation to account for the single-scattering losses.

It is emphasized that the model predicts the irradiance and not the radiant intensity. Experimentally, this means that $(A_r A_r^* + I^+)$ and I^- must be measured with wide field of view detectors.

6.0 BEAM WAVES

We consider the problem of an initially Gaussian beam illuminating a particulate medium. The propagation coefficients are either specified directly or have been derived from eqs. 58-69. Then the propagation eqs. 94-96 must be solved. The principal difficulty resides in the coupling between the forward- and the backscattered irradiance. In the present application, the coupling is treated

iteratively, first by setting $I^- = 0$ in eq. 95 and solving for I^+ and I^- in sequence, and then by substituting the I^- solution back into eq. 95 and repeating the process. Under these conditions, the equations can be solved analytically.

To reduce the number of parameters, we assume a collimated beam, i.e. $F \to \infty$, and we make the following simplifications

$$\sigma_{af} \simeq \sigma_{ab} \simeq \sigma_{afs} \simeq \sigma_{abs}, \qquad [98]$$

$$\sigma_{sf}^- \simeq \sigma_{sb}^- \simeq \sigma_{cf}^- \simeq \sigma_{cb}^-, \qquad [99]$$

which, from the defining eqs. 58-67, are expected to hold for particles larger than the wavelength. Furthermore, we define the nondimensional independent variables

$$\eta \equiv \int_o^z \sigma_t(z')dz', \qquad [100]$$

$$\rho \equiv r/w_o, \qquad [101]$$

where

$$\sigma_t \equiv \mathrm{Re}[\sigma_a - \sigma_{af} + \sigma_{cf} + \sigma_{cf}^-], \qquad [102]$$

and where w_o is the initial beam radius at 1/e in irradiance. The nondimensional propagation equations thus become

$$\frac{\partial A_r}{\partial \eta} + \frac{1}{2}(1 + i\chi) A_r - i\Delta \nabla_\rho^2 A_r = 0, \qquad [103]$$

$$\frac{\partial I^+}{\partial \eta} + \alpha I^+ - \kappa_f \nabla_\rho^2 I^+ = \beta A_r A_r^* + \tau I^-, \qquad [104]$$

$$\frac{-\partial I^-}{\partial \eta} + \alpha I^- - \kappa_b \nabla_\rho^2 I^- = \tau A_r A_r^* + \tau I^+. \qquad [105]$$

The similarity parameters are

$$\chi = \frac{\mathrm{Im}\left[\sigma_a - \sigma_{af} + \sigma_{cf} + \bar{\sigma}_{cf}\right]}{\sigma_t}, \qquad [106]$$

$$A = 1/(2\, kw_o^2\, \sigma_t), \qquad [107]$$

$$\alpha = \frac{\mathrm{Re}\left[\sigma_a - \sigma_{afs} + \bar{\sigma}_{af}\right]}{\sigma_t}, \qquad [108]$$

$$\beta = \frac{\mathrm{Re}\left[\sigma_{af} + \sigma_{cf}\right]}{\sigma_t}, \qquad [109]$$

$$\tau = \frac{\mathrm{Re}\left[\bar{\sigma}_{sb}\right]}{\sigma_t}, \qquad [110]$$

$$\kappa_f = \frac{\mathrm{Re}\left[D_f\right]}{\sigma_t w_o^2}, \qquad [111]$$

$$\kappa_b = \frac{\mathrm{Re}\left[D_b\right]}{\sigma_t w_o^2}. \qquad [112]$$

For the calculation results presented here, we have taken χ, α, β and τ to be constant throughout the medium. This constitutes a reasonable approximation if only the particle number density is allowed to change with little variations in the nature of the particles and their size distribution. The parameter A varies with σ_t but it is generally too small to make appreciable differences in the solutions and it was assumed constant. Moreover, the coefficients κ_f and κ_b increase from zero to asymptotic values in their respective transition regions near

the medium boundaries. However, since the scattered irradiance is small in the transition regions, we have approximated

$$\kappa_f \approx \kappa_b = \kappa = \text{cst} \qquad [113]$$

everywhere with little effect on the resulting solutions.

The solutions were calculated for the boundary conditions

$$A_r(o,\rho) = \exp(-\rho^2), \qquad [114]$$

$$I^+(o,\rho) = 0, \qquad [115]$$

$$I^-(\zeta,\rho) = 0, \qquad [116]$$

where ζ is the optical depth of the cloud, i.e.

$$\zeta = \int_o^Z \sigma_t\,(z')dz'. \qquad [117]$$

The solutions were calculated analytically and only the first iteration was worked out. The results are presented in Figs. 2-5 for the following set of parameters: $\mu = 0$, $A = 4.7 \times 10^{-5}$, $\alpha = \tau = 0.03$, $\beta = 0.97$ and $\kappa = 65$. These are the estimated similarity parameters for a 1.06-μm, 0.15-m-diameter laser beam propagating in an advective fog of mass loading equal to 0.5 $g(H_2O)/m^3$ with a modal particle radius of 5μm. The water droplets were assumed to be nonabsorbing.

The transmitted beam irradiance profile, i.e. $(A_r A_r^* + I^+)$, at $\eta = 0,2,4,6$ and 8 optical depths are plotted in Fig. 2. The irradiance is normalized to unity on the propagation axis ($\rho = 0$) at the transmitter ($\eta = 0$). The results show that the basic Gaussian shape of the beam is not appreciably broadened up to optical depths as large as 6.

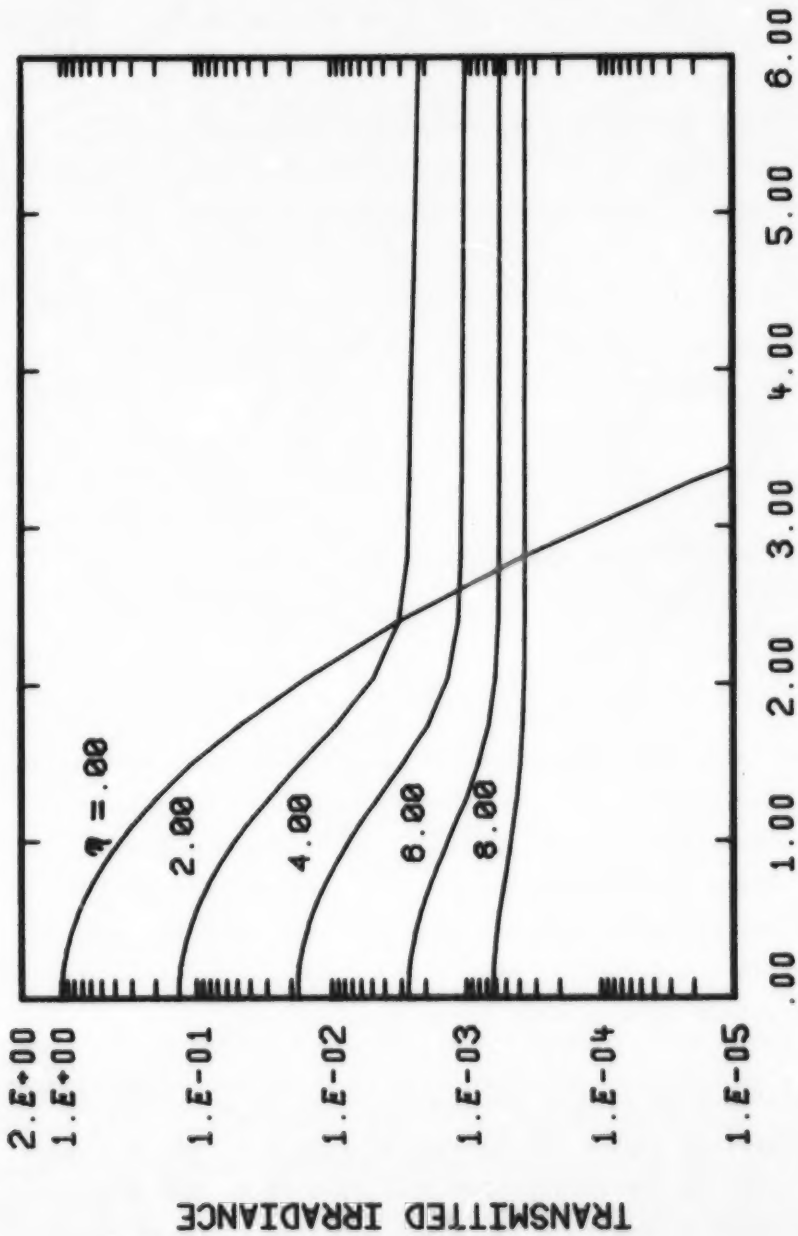

FIGURE 2 - Predicted irradiance profiles of forward-propagating beam versus normalized transverse coordinate r/w_0 for an originally Gaussian beam. η is optical depth and calculations were performed for $\mu = 0$, $\Lambda = 4.7 \times 10^{-5}$, $a = \tau = 0.03$, $s = 0.97$ and $\kappa = 65$.

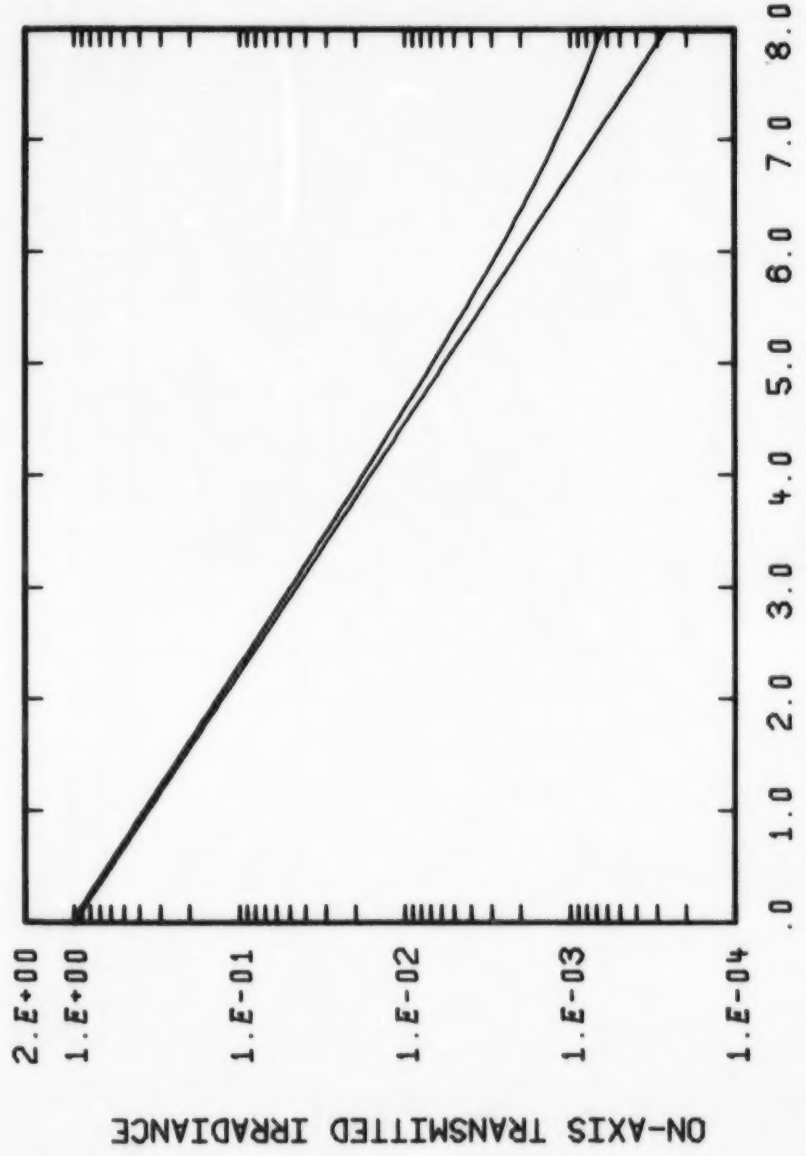

FIGURE 3 - Predicted forward-propagating on-axis irradiance as a function of optical depth η for an originally Gaussian beam. Similarity parameters as in Fig. 2. Upper curve is result of present multiple-scattering model while lower curve represents single-scattering Beer-Lambert's law under same conditions.

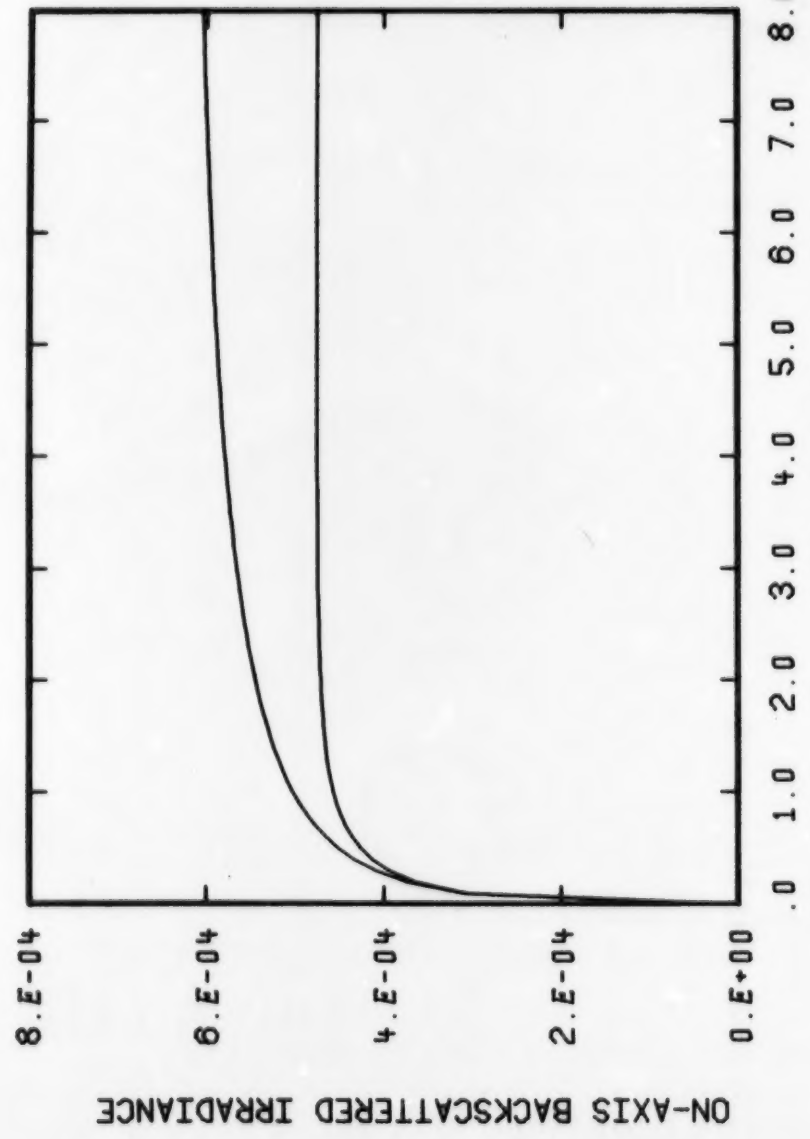

FIGURE 4 - Predicted integrated backscattered irradiance from an originally Gaussian beam propagated through a cloud of optical thickness ζ as a function of ζ. Similarity parameters as in Fig. 2. Upper curve is result of present multiple-scattering model while the lower curve represents predictions from first-order multiple-scattering version of the model.

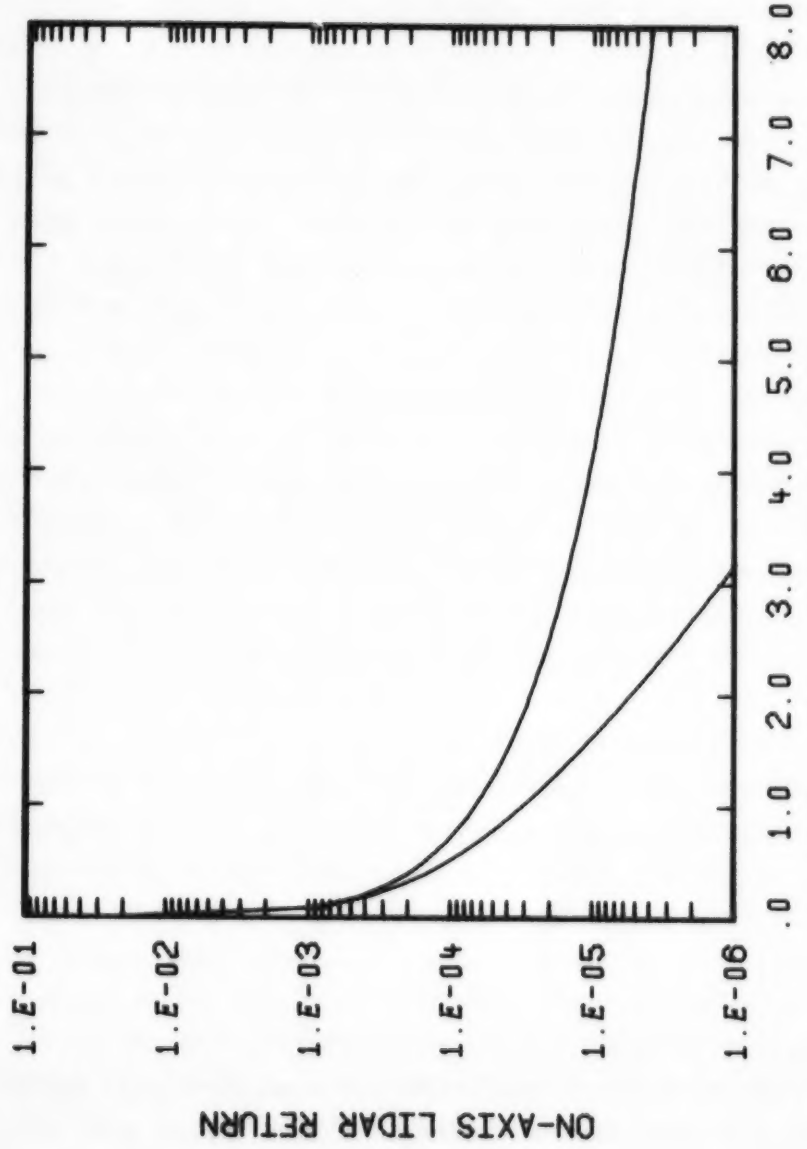

FIGURE 5 - Predicted lidar return from an originally Gaussian beam as a function of optical depth. Front end of cloud coincides with detector plane. Similarity parameters as in Fig. 2, and distinction between upper and lower curves as in Fig. 4.

This is in good agreement with the laboratory data of Smith et al. (Ref. 22). The off-axis buildup is the result of multiple scattering. At optical depth $\gtrsim 8$, the beam becomes nearly uniform as the coherent irradiance has faded to a negligible level.

The on-axis transmitted irradiance versus the optical depth is plotted in Fig. 3 and compared with the single-scattering result. The normalization is the same as in Fig. 2. The differences between the complete solution and the single-scattering solution remain small up to an optical depth of about 6 where the two curves begin to diverge. These results indicate that the scattered energy is diffused laterally with only a small fraction remaining on the line of sight. That fraction becomes important relative to the single-scattering predictions only at large optical depths, approximately 6 in the present application. Hence, as far as the on-axis transmitted signal is concerned, the effect of multiple scattering may be neglected with good accuracy unless very large optical depths are to be considered, typically greater than 6-8. This conclusion applies to on-axis detection only; for off-axis detection, the multiple-scattering effect dominates, as illustrated in Fig. 2.

The integrated backscattered irradiance from a cloud of optical thickness ζ and measured at the transmitter site is drawn as a function of ζ in Fig. 4. The normalization is the same as in the previous figures. The highest curve represents the prediction from our full model and the lowest one, from its first-order multiple-scattering version as defined earlier. The first-order multiple-scattering curve saturates very rapidly; there is virtually no increase for cloud thicknesses greater than 2. On the contrary, the return predicted by the multiple-scattering theory saturates much more slowly and at a higher level. At optical thickness 8, the curve has not yet reached its asymptotic value. These two curves are in excellent qualitative agreement with the measurements of Ref. 22.

Whereas the effects of multiple scattering were unimportant for on-axis measurements of the transmitted beam, Fig. 4 shows that they are significant for the analysis of the detected backscatter. This is even more dramatic if we consider the lidar signal, i.e. the range-gated backscatter signal, as illustrated in Fig. 5. At optical depth 3, the difference between the full multiple scattering and the first-order multiple-scattering predictions has already reached a multiplicative factor of 10 and it continues to grow with increasing optical depth. These results have great implications in the interpretation of lidar measurements. Careful comparison with well-documented data is still needed but Figs. 4 and 5 indicate that the effect of multiple scattering is potentially very important.

The calculation results depicted in Figs. 2-4 agree well with various known effects of the multiple-scattering phenomenon, in particular its greater influence on the backscatter than on the transmission measurements. These solutions were derived analytically with the help of a number of simplifying approximations stated at the beginning of this chapter. For more general applications, the propagation eqs. 103-105 can be solved numerically with no restrictions on the absorption, scattering and diffusion coefficients other than the hypothesis of homogeneity over a scale of the order of the beam diameter. The equations present no particular difficulties for a numerical solution.

7.0 PLANE WAVES

It is instructive to consider the special geometry of plane or spherical waves. This simplification allows complete solutions to be derived in closed analytic form. These analytic expressions are very useful for parametric studies. Moreover, the planar or spherical geometry represents adequately many physical situations, e.g. the planetary atmospheres, the clouds and the ocean waters illuminated by the sun.

The same simplifying approximations as in the preceding section are made. The nondimensional propagation eqs. 112-114 are adapted to planar geometry by simply neglecting the transverse gradients. We thus obtain

$$\frac{dA_r A_r^*}{d\eta} + A_r A_r^* = 0, \qquad [118]$$

$$\frac{dI^+}{d\eta} + \alpha I^+ = \beta A_r A_r^* + \tau I^-, \qquad [119]$$

$$-\frac{dI^-}{d\eta} + \alpha I^- = \tau A_r A_r^* + \tau I^+. \qquad [120]$$

Equations 118-120 form a closed set of three simultaneous, coupled ordinary differential equations. The boundary conditions are

$$A_r A_r^* (0) = 1, \qquad [121]$$

$$I^+ (0) = 0, \qquad [122]$$

$$I^- (\zeta) = 0, \qquad [123]$$

where ζ is the optical thickness of the plane-parallel scattering medium.

The set of eqs. 118-120 is identical to the four-flux theory described in Chapt. 10 of Ref. 1 where $A_r A_r^*$ is the forward collimated flux and I^+ and I^-, the forward- and backward-diffused fluxes respectively. We have simplified the problem by assuming no backward-collimated flux and making such approximations as defined by eqs. 98 and 99. These make the algebra easier but they are not fundamental to the model. Therefore, the four-flux theory is the plane-wave asymptotic form of the propagation model proposed in this report. However, contrary to the four-flux theory, which is constructed heuristically

with propagation coefficients not clearly related to the physical parameters of the particulate medium, our model is derived from Maxwell's equations and the coefficients are formally related to the medium properties.

The propagation eqs. 118-120 with the boundary conditions 121-123 are straightforward to solve. The similarity parameters are the albedo

$$\Omega = \frac{\mathrm{Re}\left[\sigma_{cf} + \sigma_{cf}^{-}\right]}{\sigma_t}, \qquad [124]$$

and the ratio of the backscattering to the total scattering coefficients

$$\Pi = \frac{\mathrm{Re}\left[\sigma_{cf}^{-}\right]}{\mathrm{Re}\left[\sigma_{cf} + \sigma_{cf}^{-}\right]}. \qquad [125]$$

With the further approximation $\sigma_{af} \ll \sigma_{cf}$, which is almost always satisfied in practical cases, the results are:

a) for the total irradiance transmitted through a cloud of optical thickness ζ

$$A_r A_r^*(\zeta) + I^+(\zeta) = \frac{2\varepsilon\, e^{-\varepsilon\zeta}}{(\delta+\varepsilon) - (\delta-\varepsilon)e^{-2\varepsilon\zeta}}, \qquad [126]$$

and b) for the integrated backscattered irradiance from a cloud of thickness ζ

$$I^-(0,\zeta) = \frac{\Pi\Omega\left[1 - e^{-2\varepsilon\zeta}\right]}{(\delta+\varepsilon) - (\delta-\varepsilon)\, e^{-2\varepsilon\zeta}}, \qquad [127]$$

where

$$\delta = (1-\Omega) + \Pi\Omega, \qquad [128]$$

$$\varepsilon^2 = (1-\Omega)\,[(1-\Omega) + 2\Pi\Omega]. \qquad [129]$$

The corresponding single-scattering (SSCT) and first-order multiple-scattering (FOMS) solutions are

$$[A_r A_r^*(\zeta)]_{SSCT} = e^{-\zeta}, \qquad [130]$$

$$[I^-(0,\zeta)]_{FOMS} = \frac{\Pi\Omega}{2}\,[1 - e^{-2\zeta}]. \qquad [131]$$

For spherical waves, we find exactly the same expressions except for the multiplicative geometric factors R^2_2 and R^2_1 on the left-hand side of eqs. 126(130) and 127(131) respectively. R_1 and R_2 are the radial positions of the centered front and back spherical boundaries of the scattering medium.

The transmitted irradiance solutions are plotted in Fig. 6 versus the cloud optical thickness ζ, for $\Pi = 0.04$ and various values of the albedo Ω. The decay rate with respect to ζ varies inversely with Ω but, in all cases, it remains smaller than for the single-scattering solution (SSCT). The latter is reached in the limit $\Omega \to 0$, i.e. when the absorption becomes dominant over the scattering.

The integrated backscatter results are displayed in Fig. 7. All the curves saturate to some asymptotic level but the required cloud thickness and the saturation level increase with Ω. If there is no absorption ($\Omega = 1$), the transmitted irradiance is eventually all reflected back for optical thicknesses much greater than $1/\Pi$. In the

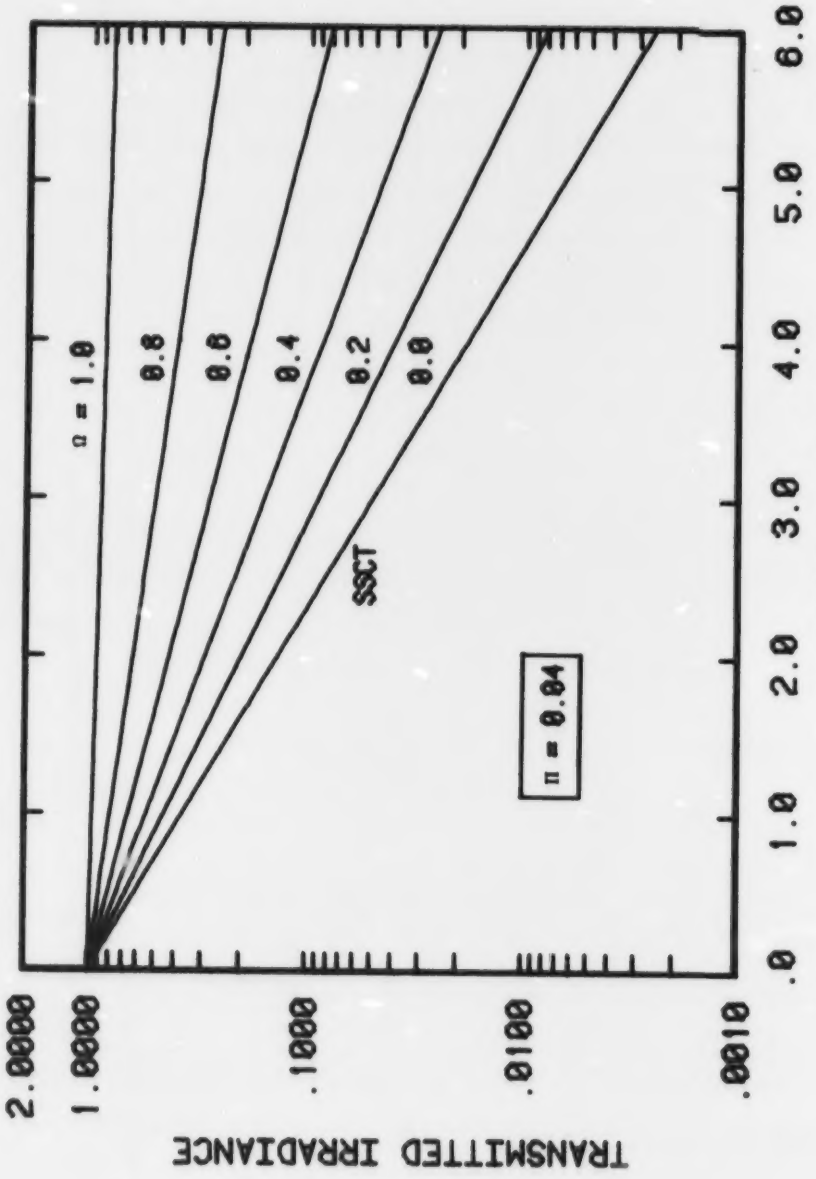

FIGURE 6 - Predicted forward-propagating irradiance in a plane-parallel geometry as a function of the optical depth η defined by eq. 100. Ω is single-scattering albedo and Π, the ratio of backscattering to the total-scattering coefficients. Curve marked SSCT represents single-scattering Beer-Lambert's law.

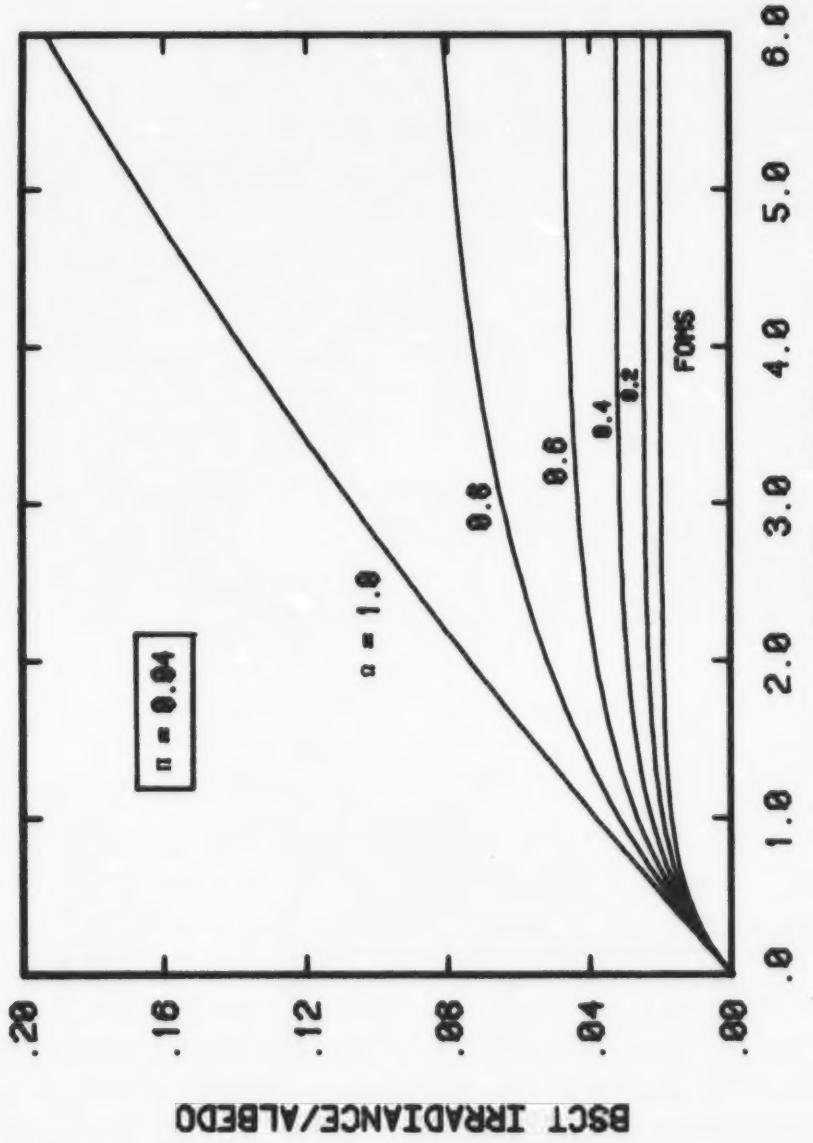

FIGURE 7 - Predicted integrated backscattered irradiance in a plane-parallel geometry. Notation as in Fig. 6 except for curve marked FONS which represents the result of first-order multiple-scattering approximation.

first-order multiple-scattering limit, the backscattered irradiance saturates quickly for $\zeta \gtrsim 2$ and at a level equal to $\Pi\Omega/2$ which represents only a small fraction of the transmitted signal.

Figures 6 and 7 show large differences between the plane-wave multiple- and single-scattering solutions. This is in agreement with the fundamental differences between the two approaches. In single scattering, the scattered energy is assumed lost whereas it is simply redistributed spatially in multiple scattering. Because of the plane-parallel geometry, the losses at one point due to spatial redistribution are compensated for by gains from the adjacent regions. Hence, the multiple-scattering solutions should indeed predict higher transmitted and backscattered irradiance levels, as illustrated by our results in Figs. 6 and 7. Moreover, it is well understood that the single-scattering solution should become more accurate as the effect of absorption increases since the absorption represents a true energy loss to propagation. This is also well verified by the predictions of our model.

An interesting physical situation is the no-absorption limit, i.e. $\Omega \to 1$. In this case, $\delta \to \Pi$, $\varepsilon \to 0$, and the transmitted and integrated backscattered irradiances become respectively

$$A_r A_r^*(\zeta) + I^+(\zeta) = \frac{1}{1+\Pi\zeta} , \qquad [132]$$

$$I^-(0,\zeta) = \frac{\Pi\zeta}{1+\Pi\zeta} . \qquad [133]$$

Bucher (Ref. 16) has shown that Monte Carlo simulations fit very well the expression

$$I_t(\zeta) = \frac{1.69}{1.42 + (1-\langle\cos\theta\rangle)\zeta} , \qquad [134]$$

for $(1-\langle\cos\theta\rangle)\zeta > 1$, where $I_t = A_r A_r^* + I^+$ and where $\langle\cos\theta\rangle$ is the average cosine of the scattering angle over the complete forward and backward directions relative to the incident axis. It is not clear how $(1-\langle\cos\theta\rangle)$ relates exactly to our parameter Π, but they both vary in the same direction with the ratio of the backscattering to the forward-scattering coefficients and they are both of the same order of magnitude, i.e. a few percent. Therefore, eqs. 132 and 134 show that our analytic solution is in good qualitative agreement with Monte Carlo data. This functional relationship was also verified in a laboratory experiment (Ref. 23).

8.0 CONCLUSION

We have derived from Maxwell's equations a propagation model for optical and infrared waves in particulate media. It has the form of simultaneous three-dimensional partial differential equations for the average amplitude and the average scattered irradiance of the forward- and backward-propagating waves. These equations involve absorption, scattering and diffusion coefficients that are formally related to the statistical properties of the particles and the surrounding medium. The model handles beams, includes all orders of scattering, and is applicable to inhomogeneous media provided the inhomogeneity scale is not smaller than the beam diameter. The main restriction is that the fraction of volume occupied by the particles to the $\frac{1}{3}$th power must be much smaller than unity, which is well verified in atmospheric applications. The polarization effects are neglected in the present version.

The propagation equations are linear and simple to solve, at least numerically. The coefficients are related to the medium properties through nonlinear equations which are difficult to deal with. In this report, only order-of-magnitude estimates of these coefficients

were obtained. The important observations, however, are that the relations do exist and that they are not coupled to the propagation problem. Thus, the coefficients can be solved independently or inferred by some other means such as experimental measurements or empirical modeling.

The solutions derived in this report are in good agreement with the present understanding of the multiple-scattering phenomenon. Closed form expressions were obtained that are useful for analytical purposes. In particular, the model provides a convenient theoretical tool for the analysis of the multiple-scattering effect on the inversion of the lidar data. This will constitute the subject of a future report.

9.0 REFERENCES

1. Ishimaru, A., "Wave Propagation and Scattering in Random Media", Vols. 1 and 2, Academic Press, New York, 1978.

2. Zuev, V.E., "Laser Beams in the Atmosphere", translated from Russian by James S. Wood, Consultants Bureau, Plenum Publishing Corp., 1982.

3. Twersky, V., "Interference Effects in Multiple Scattering by Large, Low-Refracting, Absorbing Particles", J. Opt. Soc. Am., Vol. 60, pp. 908-914, 1970.

4. Twersky, V., "Absorption and Multiple Scattering by Biological Suspensions", J. Opt. Soc. Am., Vol. 60, pp. 1084-1093, 1970.

5. Twersky, V., "Multiple Scattering of Sound by a Periodic Line of Obstacles", J. Acoust. Soc. Am., Vol. 53, No. 1, pp. 96-112, 1973.

6. Arnush, D., "Underwater Light Beam Propagation in the Small-Angle-Scattering Approximation", J. Opt. Soc. Am., Vol. 62, p. 1109, 1972.

7. Fante, R.L. "Propagation of Electromagnetic Waves through Turbulent Plasma Using Transport Theory", IEEE Trans Antennas Propag., AP-21, p. 750, 1973.

8. Hong, S.T. and Ishimaru, A., "Two-Frequency Mutual Coherence Function; Coherence Bandwidth; and Coherence Time of Millimeter and Optical Waves in Rain, Fog and Turbulence", Radio Sci., Vol. 11, p. 551, 1976.

9. Stotts, L.B., "The Radiance Produced by Laser Radiation Transversing a Particulate Multiple-Scattering Medium", J. Opt. Soc. Am., Vol. 67, p. 815, 1977.

10. Box, M.A. and Deepak, A., "Limiting Cases of the Small-Angle Scattering Approximation Solutions for the Propagation of Laser Beams in Anisotropic Scattering Media", J. Opt. Soc. Am., Vol. 71, p. 1534, 1981.

11. Tam, W.G. and Zardecki, A., "Laser Beam Propagation in Particulate Media", J. Opt. Soc. Am., Vol. 69, p. 68, 1979.

12. Tam, W.G. and Zardecki, A., "Multiple Scattering of a Laser Beam by Radiational and Advective Fogs", Optica Acta, Vol. 26, p. 659, 1979.

13. Zardecki, A. and Tam, W.G., "Iterative Method for Treating Multiple Scattering in Fogs", Can. J. Phys., Vol. 57, p. 1301, 1979.

14. Tam, W.G. and Zardecki, A., "Multiple Scattering Corrections to the Beer-Lambert Law 1: Open Detector", J. Appl. Optics, Vol. 21, p. 2405, 1982.

15. Zardecki A. and Tam, W.G., "Multiple Scattering Corrections to the Beer-Lambert Law 2: Detector with a Variable Field of View", J. Appl. Optics, Vol. 21, p. 2413, 1982.

16. Bucher, E.A., "Computer Simulation of Light Pulse Propagation for Communication through Thick Clouds", Appl. Opt., Vol. 12, p. 2391, 1973.

17. Plass, G.N. and Kattawar, G.W., "Monte Carlo Calculations of Light Scattering from Clouds", Appl. Opt., Vol. 7, p. 415, 1978.

18. Bissonnette, L. and Côté, R., "Angle of Arrival and Irradiance Statistics of Laser Beams in Turbulence", DREV R-4213/81, July 1981, UNCLASSIFIED

19. Bissonnette, L., "Focused Laser Beams in Turbulent Media", DREV R-4178/80, December 1980, UNCLASSIFIED

20. Bissonnette, L., "Modelling of Laser Beam Propagation in Atmospheric Turbulence", in "Proceedings of the Second International Symposium on Gas Flow and Chemical Lasers", J.F. Wendt, ed., Hemisphere, Washington, D.C., 1979, pp. 73-94.

21. Batchelor, G.K., "The Theory of Homogeneous Turbulence", Cambridge University Press, 1960.

22. Smith, R.B., Carswell, A.I., Houston, J.D., Pal, S.R. and Greiner, B.C., "Multiple Scattering Effects on Backscattering and Propagation of Infrared Laser Beams in Dense Military Screening Clouds", Optech Inc. Report prepared for Defence Research Establishment Valcartier, Contract No. 8SD81-00084, February 1983, UNCLASSIFIED

23. Elliot, R.A., "Wave Propagation in Particulate Media: Multiple Scattering of Optical Pulses in Scale Model Clouds", The Oregon Graduate Center, Report prepared for the Office of Naval Research, Contract No. N00014-79-C-00897, March 1983, UNCLASSIFIED

DREV R-4351/85 (UNCLASSIFIED)

Research and Development Branch, DND, Canada.
DREV, P.O. Box 8800, Courcelette, Que. G0A 1R0

"Laser Forward- and Backscattering in Particulate Media"
by L.R. Bissonnette

A model of optical and infrared wave propagation in scattering media is derived from Maxwell's equations. It allows for the calculation of the irradiance profiles of the forward- and the backward-propagating beams which result from the interaction of a coherent beam with a scattering medium. The method accounts for all orders of scattering and is applicable to inhomogeneous media. The range of validity is limited by the condition that the fractional volume occupied by the particles to the $\frac{1}{3}$th power must be much smaller than unity.

DREV R-4351/85 (UNCLASSIFIED)

Research and Development Branch, DND, Canada.
DREV, P.O. Box 8800, Courcelette, Que. G0A 1R0

"Laser Forward- and Backscattering in Particulate Media"
by L.R. Bissonnette

A model of optical and infrared wave propagation in scattering media is derived from Maxwell's equations. It allows for the calculation of the irradiance profiles of the forward- and the backward-propagating beams which result from the interaction of a coherent beam with a scattering medium. The method accounts for all orders of scattering and is applicable to inhomogeneous media. The range of validity is limited by the condition that the fractional volume occupied by the particles to the $\frac{1}{3}$th power must be much smaller than unity.

DREV R-4351/85 (UNCLASSIFIED)

Research and Development Branch, DND, Canada.
DREV, P.O. Box 8800, Courcelette, Que. G0A 1R0

"Laser Forward- and Backscattering in Particulate Media"
by L.R. Bissonnette

A model of optical and infrared wave propagation in scattering media is derived from Maxwell's equations. It allows for the calculation of the irradiance profiles of the forward- and the backward-propagating beams which result from the interaction of a coherent beam with a scattering medium. The method accounts for all orders of scattering and is applicable to inhomogeneous media. The range of validity is limited by the condition that the fractional volume occupied by the particles to the $\frac{1}{3}$th power must be much smaller than unity.

DREV R-4351/85 (UNCLASSIFIED)

Research and Development Branch, DND, Canada.
DREV, P.O. Box 8800, Courcelette, Que. G0A 1R0

"Laser Forward- and Backscattering in Particulate Media"
by L.R. Bissonnette

A model of optical and infrared wave propagation in scattering media is derived from Maxwell's equations. It allows for the calculation of the irradiance profiles of the forward- and the backward-propagating beams which result from the interaction of a coherent beam with a scattering medium. The method accounts for all orders of scattering and is applicable to inhomogeneous media. The range of validity is limited by the condition that the fractional volume occupied by the particles to the $\frac{1}{3}$th power must be much smaller than unity.

CRDV R-4351/85 (NON CLASSIFIE)

Bureau - Recherche et Développement, MDN, Canada.
CRDV, C.P. 8800, Courcelette, Qué. G0A 1R0

"Diffusion vers l'avant et rétrodiffusion de la radiation laser dans les aérosols"
par L.R. Bissonnette

On a mis au point, à partir des équations de Maxwell, un modèle de propagation des ondes optiques et infrarouges dans un milieu diffusant. Ce modèle permet de calculer les profils de l'intensité lumineuse des faisceaux se propageant vers l'avant et vers l'arrière et qui résultent de l'interaction d'un faisceau cohérent avec les particules. La méthode tient compte de tous les ordres de diffusion et peut s'appliquer aux milieux inhomogènes. Le domaine de validité est limité par la condition suivante: la fraction du volume occupé par les particules à la puissance $\frac{1}{2}$ doit être beaucoup plus petite que l'unité.

CRDV R-4351/85 (NON CLASSIFIE)

Bureau - Recherche et Développement, MDN, Canada.
CRDV, C.P. 8800, Courcelette, Qué. G0A 1R0

"Diffusion vers l'avant et rétrodiffusion de la radiation laser dans les aérosols"
par L.R. Bissonnette

On a mis au point, à partir des équations de Maxwell, un modèle de propagation des ondes optiques et infrarouges dans un milieu diffusant. Ce modèle permet de calculer les profils de l'intensité lumineuse des faisceaux se propageant vers l'avant et vers l'arrière et qui résultent de l'interaction d'un faisceau cohérent avec les particules. La méthode tient compte de tous les ordres de diffusion et peut s'appliquer aux milieux inhomogènes. Le domaine de validité est limité par la condition suivante: la fraction du volume occupé par les particules à la puissance $\frac{1}{2}$ doit être beaucoup plus petite que l'unité.

CRDV R-4351/85 (NON CLASSIFIE)

Bureau - Recherche et Développement, MDN, Canada.
CRDV, C.P. 8800, Courcelette, Qué. G0A 1R0

"Diffusion vers l'avant et rétrodiffusion de la radiation laser dans les aérosols"
par L.R. Bissonnette

On a mis au point, à partir des équations de Maxwell, un modèle de propagation des ondes optiques et infrarouges dans un milieu diffusant. Ce modèle permet de calculer les profils de l'intensité lumineuse des faisceaux se propageant vers l'avant et vers l'arrière et qui résultent de l'interaction d'un faisceau cohérent avec les particules. La méthode tient compte de tous les ordres de diffusion et peut s'appliquer aux milieux inhomogènes. Le domaine de validité est limité par la condition suivante: la fraction du volume occupé par les particules à la puissance $\frac{1}{2}$ doit être beaucoup plus petite que l'unité.

CRDV R-4351/85 (NON CLASSIFIE)

Bureau - Recherche et Développement, MDN, Canada.
CRDV, C.P. 8800, Courcelette, Qué. G0A 1R0

"Diffusion vers l'avant et rétrodiffusion de la radiation laser dans les aérosols"
par L.R. Bissonnette

On a mis au point, à partir des équations de Maxwell, un modèle de propagation des ondes optiques et infrarouges dans un milieu diffusant. Ce modèle permet de calculer les profils de l'intensité lumineuse des faisceaux se propageant vers l'avant et vers l'arrière et qui résultent de l'interaction d'un faisceau cohérent avec les particules. La méthode tient compte de tous les ordres de diffusion et peut s'appliquer aux milieux inhomogènes. Le domaine de validité est limité par la condition suivante: la fraction du volume occupé par les particules à la puissance $\frac{1}{2}$ doit être beaucoup plus petite que l'unité.